# Assessing thermostable peroxygenase cytochrome P450 enzymes as biocatalysts for selective oxidations

Oghenesivwe Osiebe, Daniel Z. Doherty and Stephen G. Bell

Discipline of Chemistry, School of Physics, Chemistry and Earth Sciences, Adelaide University, Adelaide, SA 5005, Australia

E-mail: stephen.bell@adelaide.edu.au

## Supplementary Information

### DNA sequences

DNA sequences of the P450 encoding genes were obtained in pET28a plasmid constructs (Twist Bioscience) for CYP154H1, CYP154G1 and CYP154F1 between the NcoI and XhoI restriction sites. The QE variants contained the following mutations: DNA sequence incorporating, an N-terminal 6xHis tag and a tobacco etch virus (TEV) cleavage site and the QE double mutations. QE mutations are as follows; E246Q and T247E, E238Q and T239E, E236Q and T237E for CYP154H1, CYP154F1 and CYP154G1 respectively. CYP154C35 gene and plasmid constructs were obtained as previously reported [1].

The nucleotide sequences presented below, restriction sites in bold, start and stop codons are italicised, details for CYP154C35 are available from our previous report.

**CYP154H1**

**CC*ATGG***GTGGCTCCAGCCATCACCATCACCATCACAGCAGCGGCGAAAACCTGTACTTC
CAGGGCCATATGGCATCCCCAACCGACAACCCGATCGTCTTAGATCCGTACGTGTCTGAC
TTAGAAGGGGAGCGGGAGCGGTTATATGAGGCGGGTCCTATTGCATGGGTGGAGCTGCC
CGGCGGCGTCAGAACGTGGTCCGTCACACATCATCAAGCCGCCCGTGAATTGCTTACGG
ATAGTCGGCTCTCAAAGAATATGGCTCATTGGGGAGCGTACAATCGTGGAGAAATCAGC
CCCACGTGGCCGCTTCTGTCGGTGATTCCGCCAACACCCACCAATTTGTTAGGTACGGAC
GGCGCGGAGCATAAGCGACTGAGAACGCTTACGGCACAAGCGTTCACACCACGGCGCGT
TGAGAAATTGCGTCCACGCATCAGAGAGATTACTGAGGAACTTCTGGACGCCTTAGAAG
AGCGTGCAAACGAGCCCCAAGACTTGAAGTCTGAATTTAGCTTCAAACTGCCTATGCGTG
TGATAGGGGAGCTGTACGGAGTAGAAGAGGCAGCGCATGGCCAACTGCGGAGCTTGTAC
GATAAGTTCTTTTCTTCGGTCACGCCACCAGAGGAATTCCTCGCTACACGCGAGGCGTTA
GTGCAGTTCTATACAGAGCTTATGGAACGGAAGAAGGCGAACCCGAGCGACGACTTGAC
TACAGCCTTGCTCCAAGCTAATGAGAACGGGGATCGTATGACCGACGAGGAAGTCTTAG
GTACGTTACAGATAGTCGTTGCAGCGGGACACCAGGAGACCGTCAACTTATTGACCAAT
ACGGTAAGAGCCCTGTTGCGTTTTCCGGACCAACTGGAGTTATTACGGACTGGTAAGGCT
ACGTGGGAAGCCGCAATAGAAGAGAGTTTGCGGTGGGACCCGCCTACCACAAATTTCAT
CTTCCGATTCGCTACCGAGGACATTGAATATGGTGGTGTGACAATAGCTAAGGGTGATAG
TGTTATGATCTCCTATGGGGCAATCGGTCGGGACCGTGGCCAGCACGGCGATAACCCTGA
AGTCTTTGACGTAACCAGAAAGACATCTAGCCGACACATATCCTTTGGATATGGCCCGCA
TGTTTGCCCTGGCGCGCCCCTGGCTCGACTTGAGGCTCAAGTCGCGTTACCTATGTTGTTC
GAGCGTTACCCGGACATGAAGTTAGCGGTCGACGACAGCGAACTCGTTCCTAATCCCTCG
GTGATAGTAAACAGTTTGAAGGAATTCCCGGTTATTCTCCGCCCC*TAATAG***GGTACCAAG**
**CTTCTCGAG**

**WT CYP154H1**

**CC*ATGG***GTGGCTCCAGCCATCACCATCACCATCACAGCAGCGGCGAAAACCTGTACTTC
CAGGGCCATATGGCTTCACCTACGGACAACCCGATTGTTTTGGACCCGTACGTTTCAGAC
TTAGAGGGCGAGCGGGAACGCTTGTATGAGGCGGGCCCGATAGCCTGGGTTGAACTGCC
TGGCGGAGTGCGCACGTGGTCTGTCACACACCATCAAGCTGCACGGGAGTTACTCACAG
ACTCCCGGCTGTCTAAGAATATGGCGCACTGGGGAGCCTACAATCGTGGCGAGATTTCGC
CCACGTGGCCACTTCTTAGCGTAATTCCGCCTACTCCAACGAACTTACTGGGTACTGATG
GTGCTGAGCATAAGCGCTTGCGTACTCTTACCGCACAAGCATTCACGCCACGACGGGTGG
AGAAGCTGAGACCACGTATTCGCGAGATCACGGAAGAATTACTGGATGCACTTGAGGAA
CGCGCAAACGAGCCGCAGGATCTCAAGAGCGAATTCTCATTCAAGTTGCCCATGCGCGT
GATTGGCGAATTATACGGGGTGGAAGAAGCAGCGCACGGACAACTCAGAAGTCTTTACG
ACAAGTTCTTCTCTAGTGTGACCCCGCCCGAAGAGTTCTTGGCTACACGGGAAGCCTTGG
TTCAATTCTATACCGAACTGATGGAACGTAAGAAGGCCAACCCATCAGACGACTTAACA
ACCGCATTGCTGCAAGCCAACGAAAACGGGGATCGGATGACTGACGAGGAAGTGTTAGG
TACATTGCAAATTGTAGTAGCTGCCGGCCACGAAACGACGGTGAATCTGTTAACAAACA
CAGTGCGCGCACTCCTCAGATTCCCGGACCAATTAGAGCTGCTGCGGACAGGCAAGGCG
ACCTGGGAAGCTGCCATTGAGGAGAGCCTTCGGTGGGACCCACCAACAACGAACTTTAT
CTTCAGATTTGCCACCGAGGACATAGAGTATGGTGGCGTGACCATTGCGAAGGGCGATT
CCGTAATGATTAGCTACGGCGCCATTGGCCGTGATAGAGGTCAACACGGGGACAATCCT
GAAGTGTTTGACGTCACTCGTAAGACCTCTAGTCGTCATATTAGTTTCGGGTACGGGCCC
CACGTGTGTCCAGGCGCGCCTTTGGCTCGCCTTGAAGCCCAGGTAGCGTTACCTATGCTG
TTCGAGCGCTACCCGGACATGAAGCTCGCGGTTGACGACTCTGAGCTTGTGCCTAATCCG
TCCGTTATCGTTAATTCATTAAAAGAGTTTCCAGTTATTTTACGTCCG*TAATAG***GGTACCA**
**AGCTT**

**CYP154F1 QE**

***CCATGG***GTGGCTCCAGCCATCACCATCACCATCACAGCAGCGGCGAAAACCTGTACTTCC
AGGGCCATATGGCCGCTGTTCCTGAGCCCATAGTTCTGGTTCCGGGAAAGAGTAGAGAG
CAAGCCCTTCAGCTTCGCGAGGCCGGACCCCTGGCACGCGTTGTTGTAGAAGGTCTCGAA
GTTTGGGCCCTGACTCACGACCGGGAATTACGCGAGGCTCTGATCGACCCGCGGTTCCGT
CGCAACTGGAGAACTTGGAGAGCTTTAAATGAAGGTGAGGTGGCAACCGATCACCCTGT
TGCTGCAATGGTTTATCTTGACAACATGCTGACCGTTGACGGAGAGGCACACCGTCGAAT
GCGTTCCCCAGTGGCGCAAGCGTTCACGCCCCGTCGTGTGGAGCTTTTACGACCTCGCGT
GACTGAGATTGTTAACGCATTGTTGGACCAATTAGCCGAGCGTGACGGCACTGTTGATTT
CAAGACAGAGTTTGCTTATCCACTGTCCATGCGCGTTTTCAGCGCATTGTTCGGCATTCCC
GAGCGGGATCATGGACGCATGCAGCAAATGGTAAACACCGCCTTTTCCCCGTCCTCACCA
GAGGAAGTTCGAGCCATGCGCGAAGAGCTGGATGCTTTTCTCGATGAGTTGATCGAGGA
TAAGCGCCGTTCACCTGGGGAAGATCTGACCTCAGCACTCGTTACCGCGACAGACGAGG
AACATAAGTTGAGTGACGCAGAGTTGAGAGATACTTTGTGGTTACTTGTAACTGCCGGCT
TCCAAGAAACATCGTCCGCTTTAGCTAATGCCGTACAAACTCTTTTGACTCACCCAGACC
AACTCGCTCATTTGCGATCGGGCTCAATAGCGTGGGAAGACGCGATAGAGGAAGTTTTG
CGCCAGTCCAGCAGTGTAGCAACTCTGCCATTCTTATTTGCAGCAGAAGACGTGCAGATT
GGCGACCGTACCATCAGAGCTGGTGAACCTGTCCTTTTAGCGTATCTGGCTGCGAACCTG
GACGTCGAGCGATATGGTGAGGATGCTGCAGAGTTCGACGCAACTCAATCACGTCCACG
ACACTTGGCGTTCGGTCACGGGCCCCACACGTGTTTAGGGGCTGCCCTGGCACGACTGGA
AATGGAAGTTGCTCTTACGACACTTTTCACAGAGTTCCCTGAGGTGTCTTTAGCAGAGGG
TGAGGCGCCAAGACTGGAATCAGTATTCATCCACGCCCCTGCAGCGCTCCCTATTCGCCT
TGGACCGCGTCGTACGGCCGCC*TAATAG***GGTACCAAGCTTCTCGAG**

**WT CYP154F1**

***CCATGG***GTGGCTCCAGCCATCACCATCACCATCACAGCAGCGGCGAAAACCTGTACTTCC
AGGGCCATATGGCGGCCGTACCGGAACCGATCGTACTCGTCCCAGGTAAATCTCGCGAA
CAGGCTTTGCAATTGCGAGAAGCGGGGCCGTTAGCCAGAGTAGTAGTCGAGGGGCTTGA
GGTGTGGGCATTAACACATGATCGCGAGTTGCGTGAAGCATTGATTGATCCACGCTTTCG
GCGGAATTGGCGAACCTGGCGCGCCCTGAACGAGGGAGAAGTCGCTACTGACCATCCGG
TGGCCGCGATGGTGTACCTGGATAATATGCTCACTGTGGATGGTGAAGCTCATCGACGTA
TGCGCAGTCCGGTCGCTCAGGCTTTTACCCCACGCCGCGTAGAACTCCTGCGCCCCCGAG
TAACCGAAATCGTCAATGCCCTGCTCGATCAGCTGGCAGAACGGGATGGGACCGTAGAC
TTTAAAACTGAATTCGCCTACCCCCTTTCTATGAGAGTGTTTTCAGCGCTCTTTGGTATCC
CTGAACGCGACCACGGTCGAATGCAACAGATGGTCAATACAGCTTTCTCGCCATCTAGTC
CGGAAGAGGTCCGTGCTATGCGTGAGGAACTCGACGCCTTCTTGGACGAATTAATTGAA
GACAAACGTCGCTCCCCGGGTGAGGACTTAACGAGCGCTTTAGTAACTGCCACCGATGA
AGAGCACAAACTGTCAGATGCCGAACTGCGCGACACATTATGGCTCCTGGTCACCGCTG
GTTTTGAAACTACCAGTTCAGCGCTGGCAAACGCAGTGCAGACGTTACTGACCCATCCCG
ATCAGTTAGCACACTTACGGAGCGGAAGCATTGCATGGGAAGATGCAATCGAAGAGGTG
TTACGGCAAAGTAGTTCTGTCGCCACCCTTCCCTTTCTTTTCGCCGCCGAGGATGTTCAAA
TCGGTGATCGCACGATTCGGGCAGGCGAGCCAGTACTGCTGGCTTACTTAGCAGCTAATT
TGGATGTAGAACGCTACGGCGAAGACGCAGCGGAATTTGATGCTACACAGTCTCGCCCG
CGTCATCTTGCTTTTGGCCACGGTCCGCATACCTGCCTTGGTGCGGCGTTAGCTCGTCTCG
AAATGGAAGTGGCGTTAACTACCCTCTTTACCGAATTTCCCGAAGTCAGTCTGGCTGAAG
GAGAAGCCCCGCGTTTGGAGAGCGTCTTTATTCATGCGCCCGCCGCCTTGCCGATCAGAC
TGGGGCCTCGCAGAACCGCTGCAGGTACC*TAATAG***AAGCTTCTCGAG**

**CYP154G1**

***CCATGG***GTGGCTCCAGCCATCACCATCACCATCACAGCAGCGGCGAAAACCTGT
ACTTCCAGGGCCATATGAGCTCACCGGCACCTCAGATAGTACTCGATACAGAGC
GCGGTTTGACGGAAGCCGACATCCACGCTCTTGCGGAGCACGGTCCCGTTGTGCG
GTTATCAGTTATGGGACTTGATGTCTGGGCCGTCACTGGTTACGAAGAGCTGAGA
ACGCTCATGGCGGACCCCGAAGTGAAGCGTGGTGTCGAGCACTGGACGGCAGTC
GCTCAAGGTAAAGTACCCGCCGAGCACCCTCTCGTAAAGCTCGTGAGTATGGGC
TCAATGCTTAGTAAGAACCCGCCTGAACATACCCGTTTACGTCGTTTAGTTCAAC
ATGCCTTTACGACGCGACGCGTAGAAGGCTTACGTCCGGTGGTGCAAGAGCTGA
CGCGCGCTTGTCTGGACCGGATAGACGCTTCTCAACCCTTCGACATCAATGCGGC
GCTGTCGCACCCGGTGCCCGTGGGAGTTATTGGGCGCTTATTGGGTATACCTGAA
ACCGATCAACCCGCTTTGGACTCTTTGGTTACACGTCTTCTGAGCGGCACCGACG
CTACTGTACACGAGGAGTTATACGCTTACGTGGCTGCAATGGTTGCAGCGAGAC
GCGAGCAACCGGACGACGGTCTGATCTCCGCGCTCCTTCATGTACATGACGACG
ACGGTTCCACCTTGAGCGAAGAGGATCTTATGTGGACAGTCGTCTTGCTTGTTGA
CGCTGGATTCCAAGAGACAGTCGGACAGATAAGTAACTCCGTAAGATTGTTGTT
GGAGCACCCAGACCAATTGGCGCTGGTGACTTCTGGTGAAGTACCGTGGGAACG
CGCGGTTGAAGAGTGCTTGCGTCATACGGCTTCGGTTGTCATGCTGCCGTTCTGC
TTCCCGACACGAGAGAAAGAACTTGGCGGGTACACCATCGGTGCTGGCGAACCG
GTTATGATGGTATACGGAGCCGCAAACCGAGACAGTCGCGTTCATGCTGCGCCC
AAGGTCTTTGACGTTACCCGTTCTGACTCGCGTCACATTACTTTCGGCCACGGCC
CGCACCATTGTTTAGGTGCACCGCTGGCACGGCTGGAATTGAACGTGGTGCTGCC
TGAACTGTTCGCACGTTTCCCAAAATTAGCACTGGCAGAACGAGACATACCACG
CGTCAAATCCCTGTTCGTGAATCGCCCTTCTGAGTTATGGGTCACAGCTGGGATG
GGT*TAATAG***GGTACCAAGCTTCTCGAG**

Translated amino acid sequence: N-terminal 6xHis Tag, TEV cleavage and start Met are italicised, QE mutations are highlighted.

**CYP154H1QE**

*M*GGSS*HHHHHH*SSG*ENLYFQG*H*M*ASPTDNPIVLDPYVSDLEGERERLYEAGPIAWVE
LPGGVRTWSVTHHQAARELLTDSRLSKNMAHWGAYNRGEISPTWPLLSVIPPTPTNL
LGTDGAEHKRLRTLTAQAFTPRRVEKLRPRIREITEELLDALEERANEPQDLKSEFSF
KLPMRVIGELYGVEEAAHGQLRSLYDKFFSSVTPPEEFLATREALVQFYTELMERKK
ANPSDDLTTALLQANENGDRMTDEEVLGTLQIVVAAGH**QE**TVNLLTNTVRALLRFP
DQLELLRTGKATWEAAIEESLRWDPPTTNFIFRFATEDIEYGGVTIAKGDSVMISYGA
IGRDRGQHGDNPEVFDVTRKTSSRHISFGYGPHVCPGAPLARLEAQVALPMLFERYP
DMKLAVDDSELVPNPSVIVNSLKEFPVILRP

**CYP154F1QE**

*M*GGSS*HHHHHH*SSG*ENLYFQG*H*M*AAVPEPIVLVPGKSREQALQLREAGPLARVVVE
GLEVWALTHDRELREALIDPRFRRNWRTWRALNEGEVATDHPVAAMVYLDNMLT
VDGEAHRRMRSPVAQAFTPRRVELLRPRVTEIVNALLDQLAERDGTVDFKTEFAYPL
SMRVFSALFGIPERDHGRMQQMVNTAFSPSSPEEVRAMREELDAFLDELIEDKRRSP
GEDLTSALVTATDEEHKLSDAELRDTLWLLVTAGF**QE**TSSALANAVQTLLTHPDQL
AHLRSGSIAWEDAIEEVLRQSSSVATLPFLFAAEDVQIGDRTIRAGEPVLLAYLAANL
DVERYGEDAAEFDATQSRPRHLAFGHGPHTCLGAALARLEMEVALTTLFTEFPEVSL
AEGEAPRLESVFIHAPAALPIRLGPRRTAA

**CYP154G1QE**

*M*GGSS*HHHHHH*SSG*ENLYFQG*H*M*SSPAPQIVLDTERGLTEADIHALAEHGPVVRLSV
MGLDVWAVTGYEELRTLMADPEVKRGVEHWTAVAQGKVPAEHPLVKLVSMGSM
LSKNPPEHTRLRRLVQHAFTTRRVEGLRPVVQELTRACLDRIDASQPFDINAALSHPV
PVGVIGRLLGIPETDQPALDSLVTRLLSGTDATVHEELYAYVAAMVAARREQPDDGL
ISALLHVHDDDGSTLSEEDLMWTVVLLVDAGF**QE**TVGQISNSVRLLLEHPDQLALVT
SGEVPWERAVEECLRHTASVVMLPFCFPTREKELGGYTIGAGEPVMMVYGAANRDS
RVHAAPKVFDVTRSDSRHITFGHGPHHCLGAPLARLELNVVLPELFARFPKLALAER
DIPRVKSLFVNRPSELWVTAGMG

Wild type protein sequence for CYP154H1, CYP154F1 and CYP154G1

>WP_011293225.1 **CYP154H1** *Thermobifida fusca*
MASPTDNPIVLDPYVSDLEGERERLYEAGPIAWVELPGGVRTWSVTHHQAARELLT
DSRLSKNMAHWGAYNRGEISPTWPLLSVIPPTPTNLLGTDGAEHKRLRTLTAQAFTP
RRVEKLRPRIREITEELLDALEERANEPQDLKSEFSFKLPMRVIGELYGVEEAAHGQL
RSLYDKFFSSVTPPEEFLATREALVQFYTELMERKKANPSDDLTTALLQANENGDRM
TDEEVLGTLQIVVAAGHETTVNLLTNTVRALLRFPDQLELLRTGKATWEAAIEESLR
WDPPTTNFIFRFATEDIEYGGVTIAKGDSVMISYGAIGRDRGQHGDNPEVFDVTRKTS
SRHISFGYGPHVCPGAPLARLEAQVALPMLFERYPDMKLAVDDSELVPNPSVIVNSL
KEFPVILRP

>MBO2529096.1 **CYP154F1** *Thermobifida fusca*
MAAVPEPIVLVPGKSREQALQLREAGPLARVVVEGLEVWALTHDRELREALIDPRFR
RNWRTWRALNEGEVATDHPVAAMVYLDNMLTVDGEAHRRMRSPVAQAFTPRRVE
LLRPRVTEIVNALLDQLAERDGTVDFKTEFAYPLSMRVFSALFGIPERDHGRMQQMV
NTAFSPSSPEEVRAMREELDAFLDELIEDKRRSPGEDLTSALVTATDEEHKLSDAELR
DTLWLLVTAGFETTSSALANAVQTLLTHPDQLAHLRSGSIAWEDAIEEVLRQSSSVA
TLPFLFAAEDVQIGDRTIRAGEPVLLAYLAANLDVERYGEDAAEFDATQSRPRHLAF
GHGPHTCLGAALARLEMEVALTTLFTEFPEVSLAEGEAPRLESVFIHAPAALPIRLGP
RRTAA

>WP_159055991.1 **CYP154G1** *Thermobifida fusca*
MSSPAPQIVLDTERGLTEADIHALAEHGPVVRLSVMGLDVWAVTGYEELRTLMADP
EVKRGVEHWTAVAQGKVPAEHPLVKLVSMGSMLSKNPPEHTRLRRLVQHAFTTRR
VEGLRPVVQELTRACLDRIDASQPFDINAALSHPVPVGVIGRLLGIPETDQPALDSLVT
RLLSGTDATVHEELYAYVAAMVAARREQPDDGLISALLHVHDDDGSTLSEEDLMW
TVVLLVDAGFETTVGQISNSVRLLLEHPDQLALVTSGEVPWERAVEECLRHTASVVL
LPFCFPTREKELGGYTIGAGEPVMMVYGAANRDSRVHAAPKVFDVTRSDSRHITFGH
GPHHCLGAPLARLELNVVLPELFARFPKLALAERDIPRVKSLFVNRPSELWVTAGMG

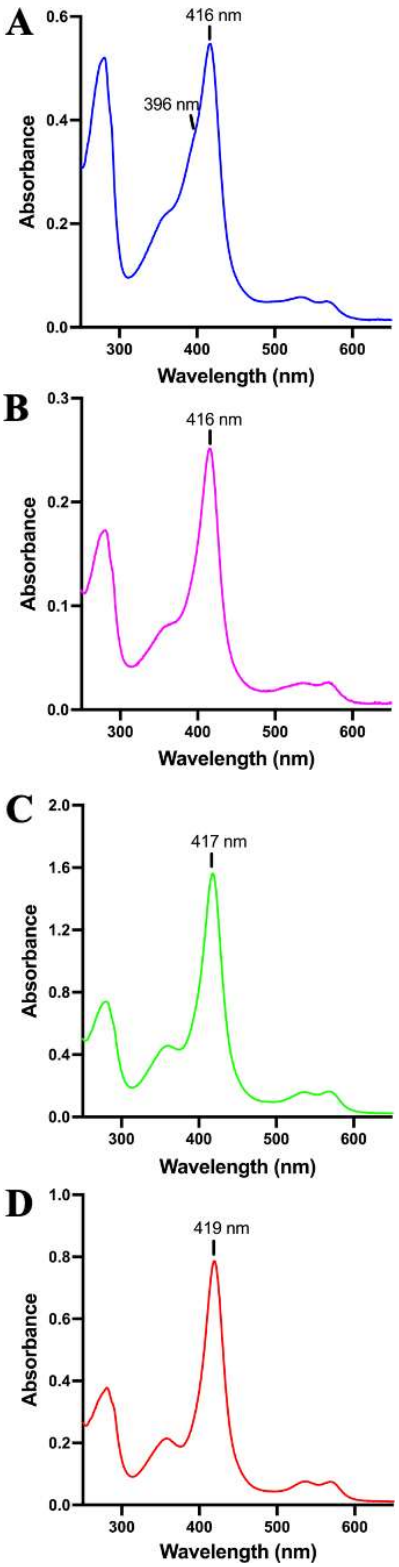



**Fig. S1** UV-Vis absorbance spectra of CYP154 enzymes after purification. (**A**) CYP154H1QE (blue). (**B**) WT CYP154H1 (pink). (**C**) CYP154G1QE (green). (**D**) CYP154F1QE (red)

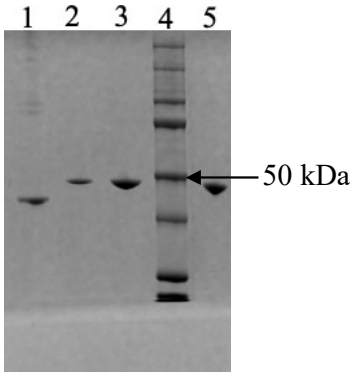



**Fig. S2** SDS-PAGE analysis of purified enzymes from *T. fusca*. Lane 1. CYP15G1QE (45.9 kDa), lane 2. CYP154H1QE (48.3 kDa), lane 3. CYP154F1QE (47.3 kDa), lane 4. Precision plus ladder (Bio-Rad), lane 5. WT CYP154H1 (48.3 kDa)

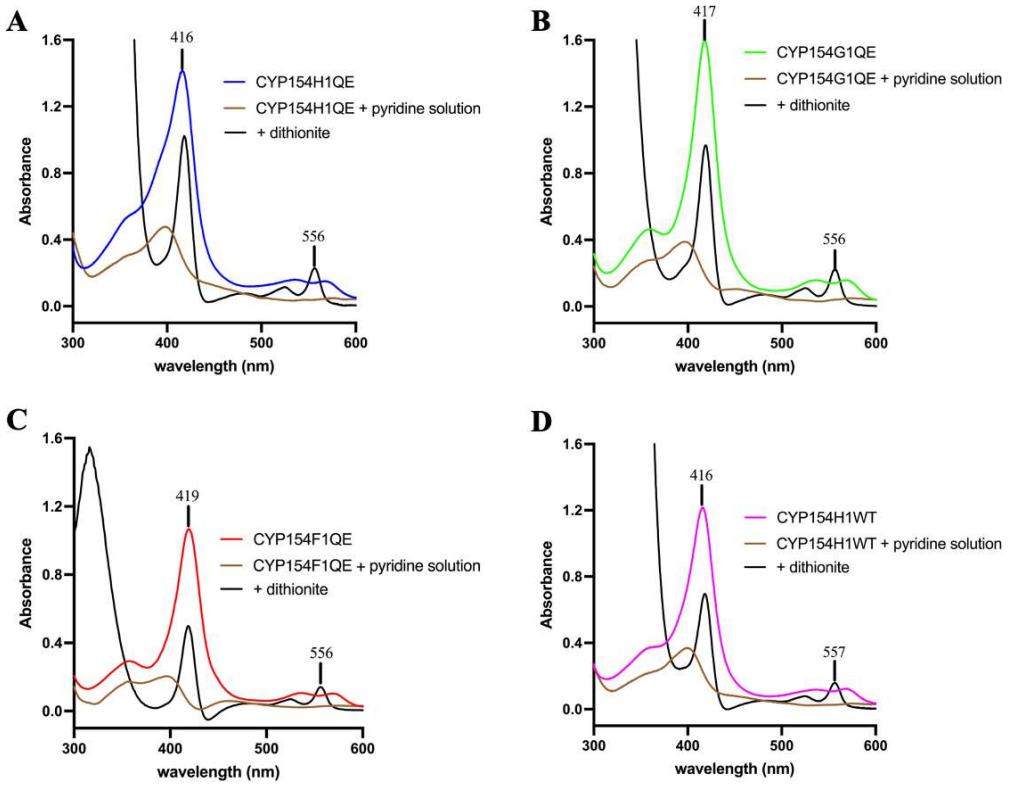
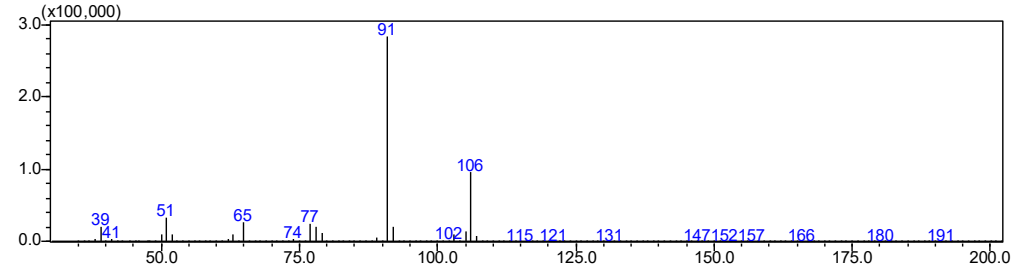
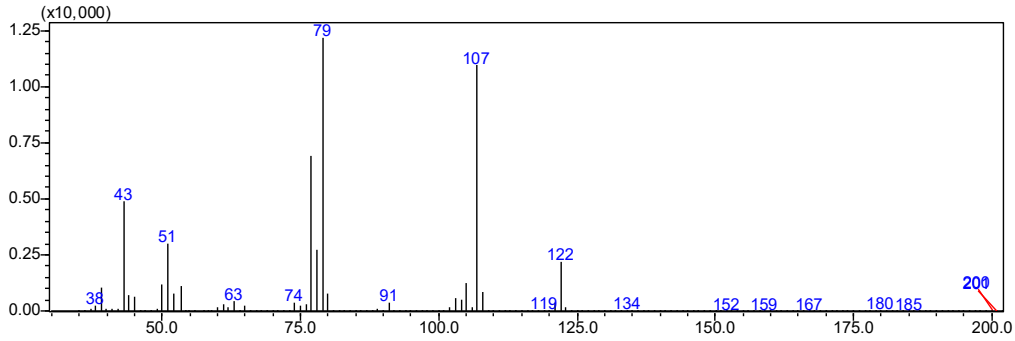


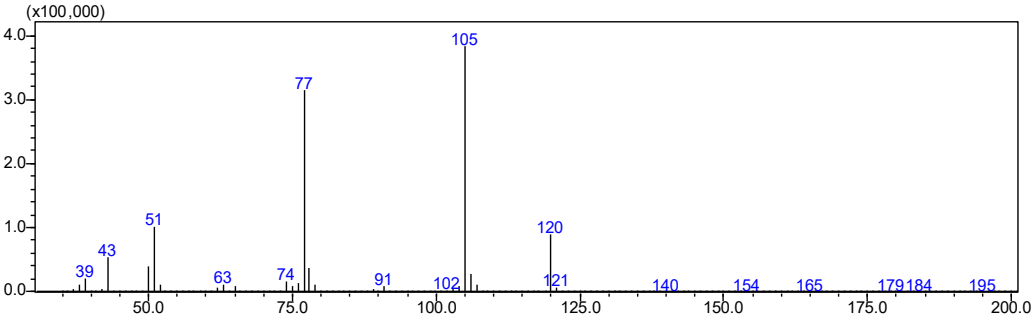

**Fig. S3** UV-Vis spectra for the determination $\varepsilon_{Soret}$ of CYPs from *T. fusca* through pyridine hemochromogen generation. (**A**) CYP154H1QE (blue). (**B**) CYP154G1QE (green) (**C**). CYP154F1QE (red). (**D**) WT CYP154H1 (pink). Ferric enzymes treated with alkaline pyridine solution (brown) and reduced pyridine hemochromagen (black)




ethylbenezene RT 3.44 min




1-phenylethanol RT 7.35 min [2, 3].




1-phenylethanone RT 7.41 min [3].

**Fig. S4** The mass spectra of generated products from ethylbenzene oxidation by CYP154 enzymes

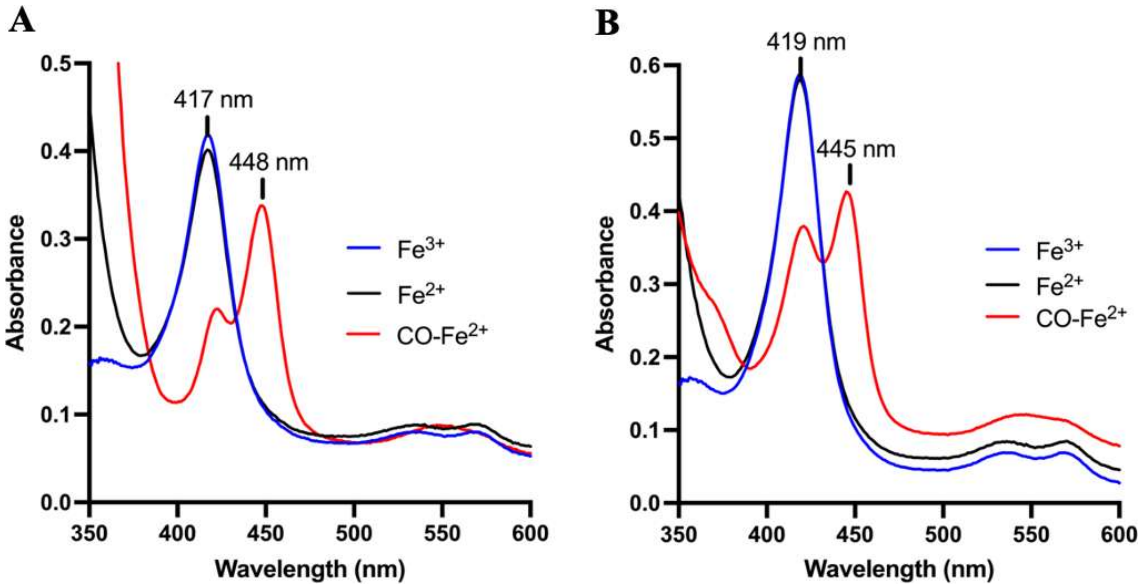



**Fig. S5** UV-Vis absorbance spectra of the ferrous CO-bound complex of CYP154 variants from *T. fusca*. (**A**) CYP154G1QE. (**B**) CYP154F1QE. The ferric (blue), ferrous (black) and ferrous-CO-bound (red) spectra are shown

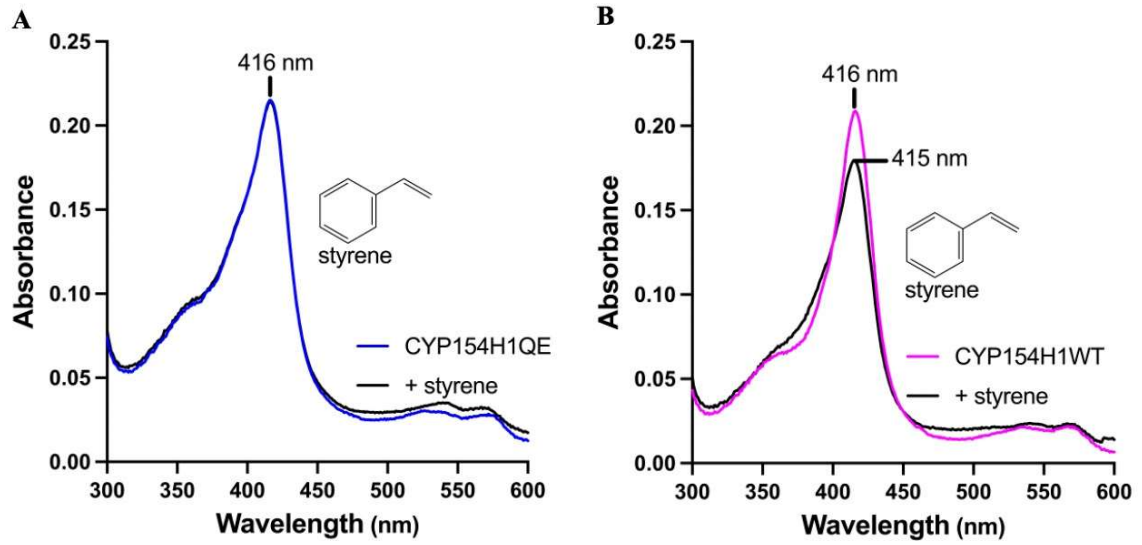



**Fig. S6** UV-Vis absorbance spectra of selected substrate free and substrate-bound CYPs. (**A**) CYP154H1QE (blue) and (**B**) WT CYP154H1 (pink) substrate-bound enzymes (black). The mixture contained 2 µM of the enzyme and 1 mM styrene

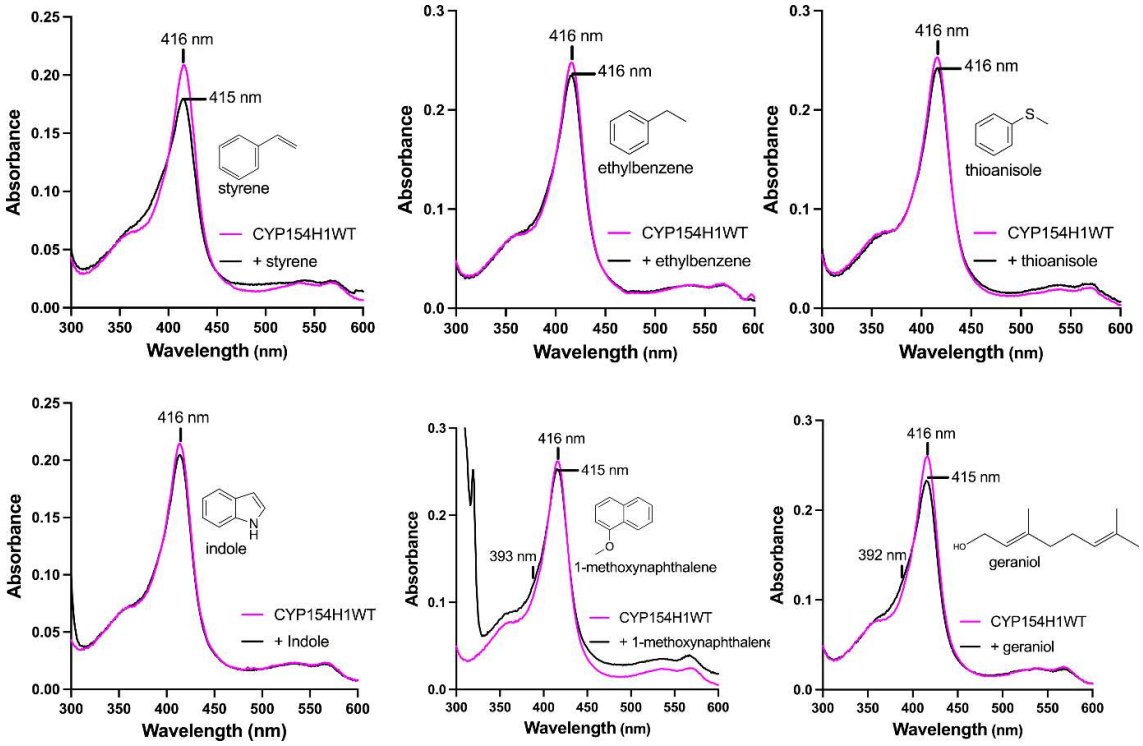



**Fig. S7** UV-Vis absorbance spectra of substrate-free and substrate-bound WT CYP154H1 with ethylbenzene, thioanisole, styrene, indole, 1-methoxynaphthalene and geraniol. Substrate-free WT CYP154H1 (pink) and substrate-bound enzyme (black)

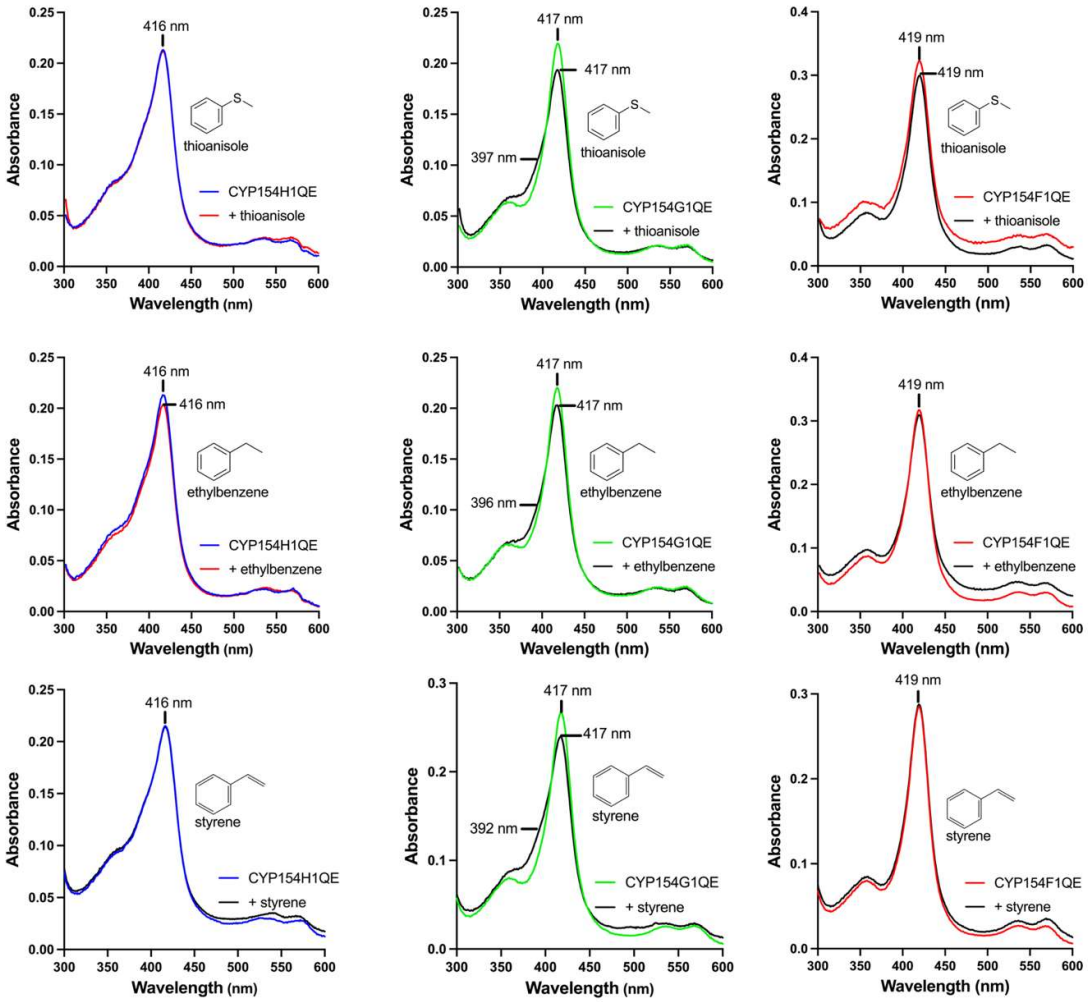



**Fig. S8** UV-Vis absorbance spectra of substrate-free CYPs and substrate-bound CYPs with ethylbenzene, thioanisole and styrene. CYP154H1QE (blue) CYP154G1QE (green) and CYP154F11 (red) and substrate-bound enzymes (black)

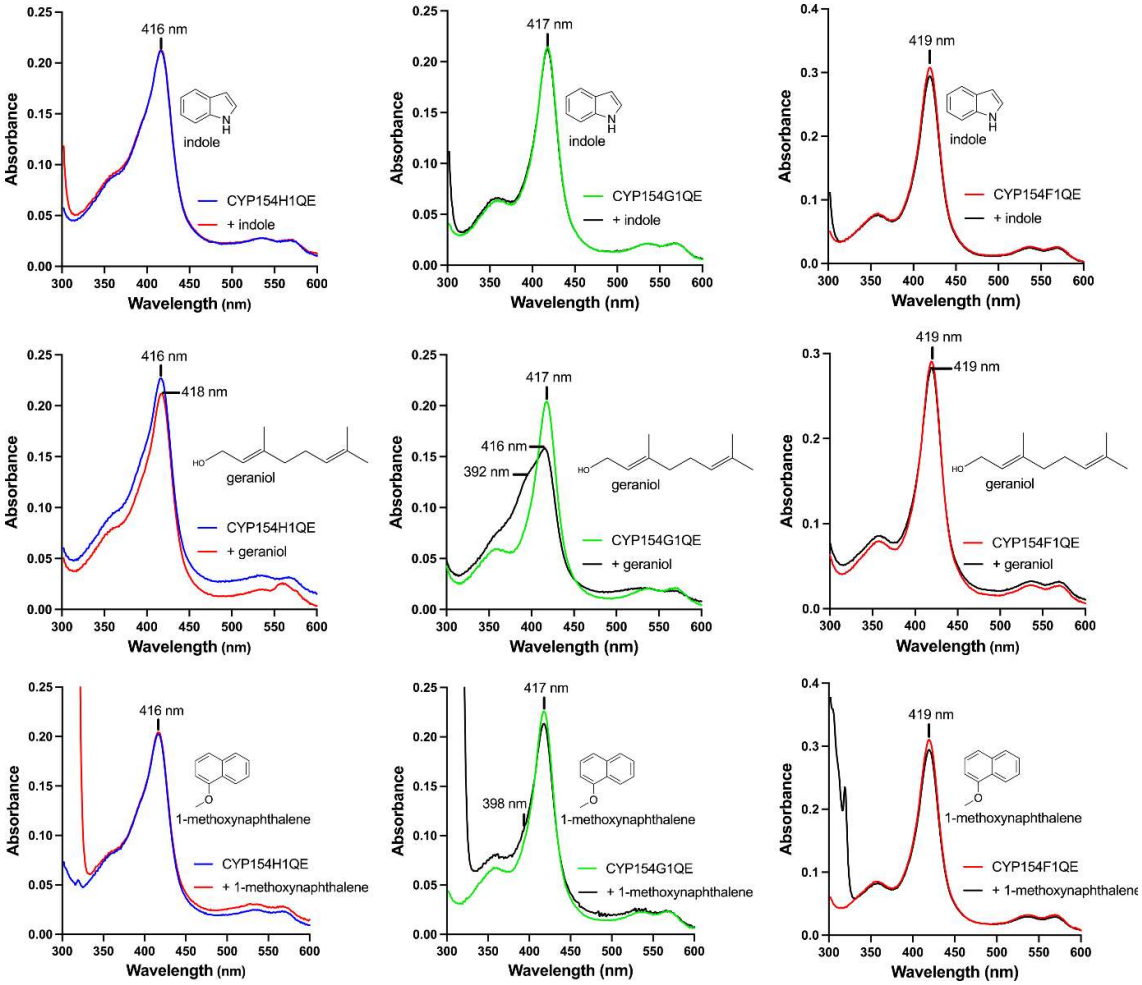



**Fig. S9** UV-Vis absorbance spectra of substrate-free CYPs and substrate-bound CYPs with indole, geraniol and 1-methoxynaphthalene. CYP154H1QE (blue) CYP154G1QE (green) and CYP154F11 (red) and substrate-bound enzymes (black)

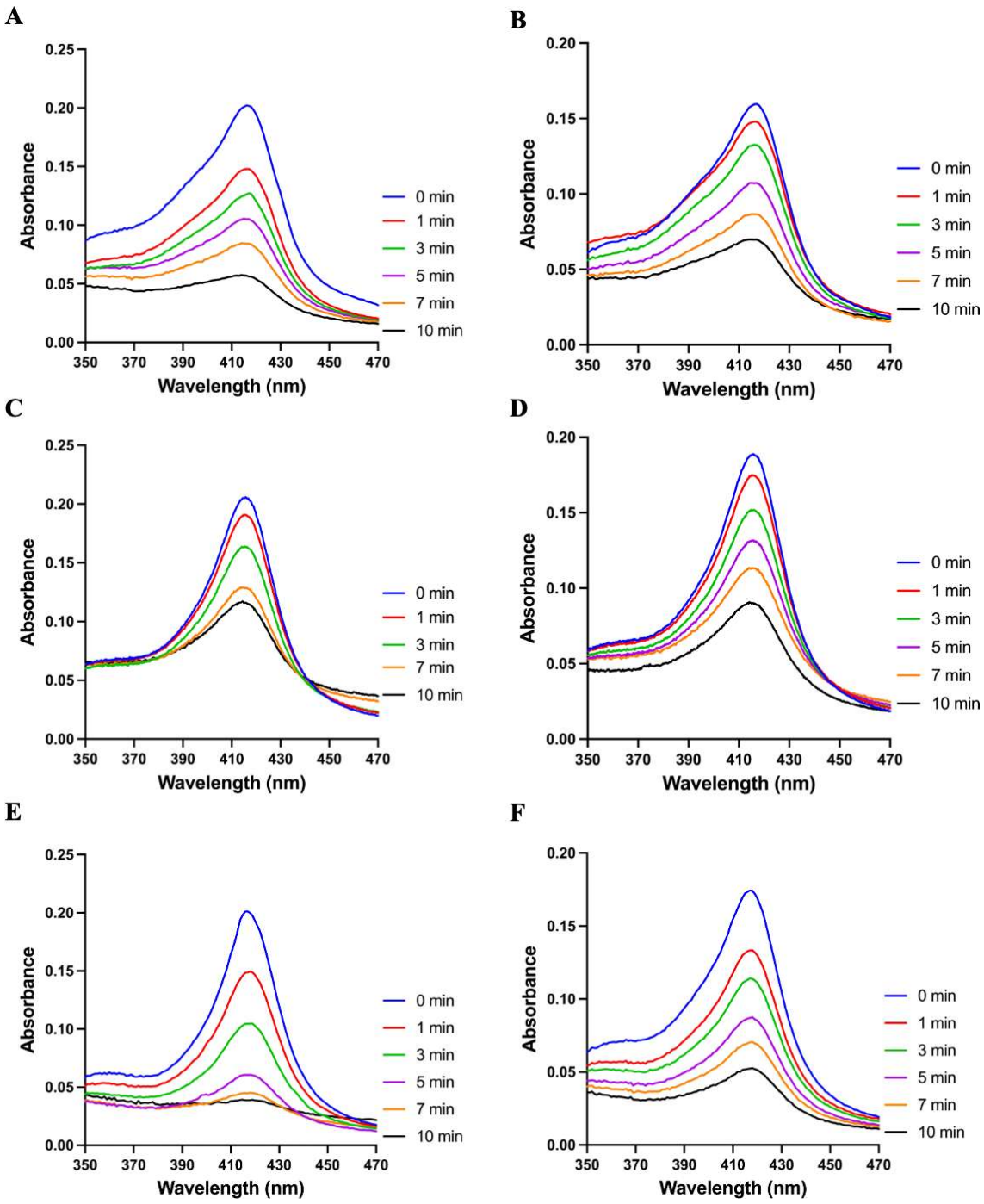



**Fig. S10** UV-Vis absorbance spectra of CYP154 enzymes in the presence of hydrogen peroxide. The heme bleaching with 10 mM $H_2O_2$, in the presence and absence of substrate was monitored over time. (**A**) The UV-Visible absorbance of CYP154H1QE in the absence of substrate and (**B**) in the presence of 1 mM styrene. (**C**) WT CYP154H1 in the absence of substrate and (**D**) in the presence of 1 mM styrene. (**E**) CYP154G1QE in the absence of substrate and (**F**) in the presence of 1 mM styrene. The reaction mixture contained 2 µM of the respective enzymes and 10 mM $H_2O_2$

**Table S1.** The rates of heme bleaching of CYPs CYP154H1QE, CYP154G1QE, CYP154F1QE and WT CYP154H1 in the presence in 1 mM substrate (styrene or geraniol) and 10 mM $H_2O_2$.

| Enzyme | Initial rate of heme destruction (ΔA/min) | Rate of heme bleaching due to 10 mM $H_2O_2$ (μm/min) |
|---|---|---|
| CYP154H1QE | -0.0069 | -0.064 |
| CYP154G1QE | -0.0089 | -0.074 |
| CYP154F1QE | -0.0041 | -0.032 |
| WT CYP154H1 | 0.0075 | -0.058 |

**Table S2.** The rates of heme bleaching of CYPs CYP154H1QE, CYP154F1QE CYP154G1QE and WT CYP154H1 in 10 mM $H_2O_2$ without substrate

| Enzyme | Initial rate of heme destruction (ΔA/min) | Rate of heme bleaching due to 10 mM $H_2O_2$ (μm/min) |
|---|---|---|
| CYP154H1QE | -0.013 | -0.12 |
| CYP154G1QE | -0.019 | -0.16 |
| CYP154F1QE | -0.0078 | -0.06 |
| WT CYP154H1 | -0.011 | -0.085 |

The rate of heme bleaching for the enzymes was determined using $\varepsilon_{416}$ 108 $mM^{-1}\,cm^{-1}$, $\varepsilon_{417}$ 120 $mM^{-1}\,cm^{-1}$, $\varepsilon_{419}$ 130 $mM^{-1}\,cm^{-1}$ and $\varepsilon_{416}$ 129 $mM^{-1}\,cm^{-1}$, for CYP154H1QE, CYP154G1QE, CYP154F1QE and WT CYP154H1 respectively. The linear portion of the curve was used to estimate the initial rate of bleaching.

**Standard plots for HPLC and GCMS quantitation**

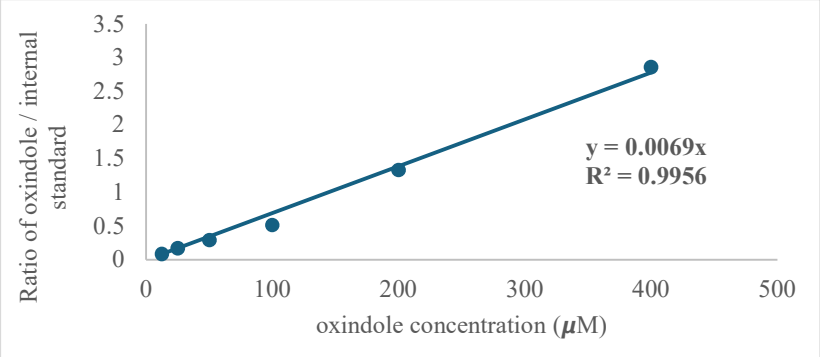



**Fig. S11** A HPLC calibration curve for the quantitation of oxindole. The curve was constructed using oxindole between 12.5-500 µM. The calibration factor is 0.0069 $\mu M^{-1}$. Isatin standards had a ratio of 0.61 when compared to oxindole standards

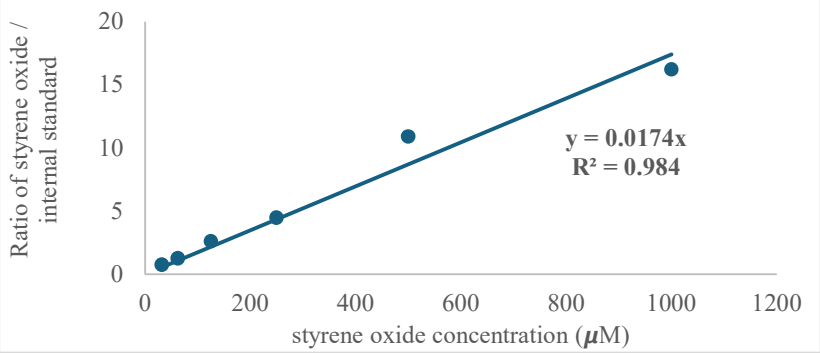



**Fig. S12** A GCMS calibration curve for the quantitation of styrene oxide. The curve was constructed using styrene oxide between 32.25-1000 µM. The calibration factor is 0.0174 $\mu M^{-1}$

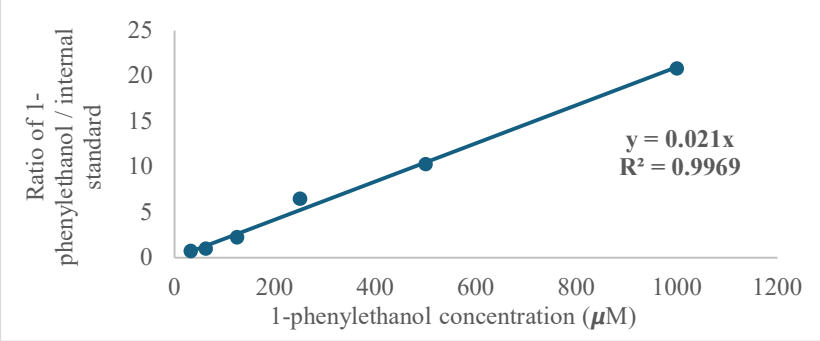



**Fig. S13** A GCMS calibration curve for the quantitation of 1-phenylethanol. The curve was constructed using 1-phenylethanol between 32.25-1000 µM. The calibration factor is 0.021 $\mu M^{-1}$

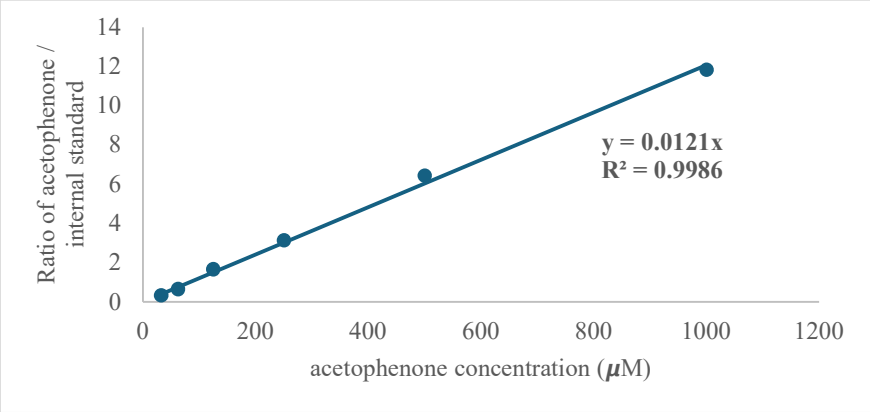



**Fig. S14** A GCMS calibration curve for the quantitation of acetophenone. The curve was constructed using acetophenone between 32.25-1000 µM. The calibration factor is 0.0121 $\mu M^{-1}$

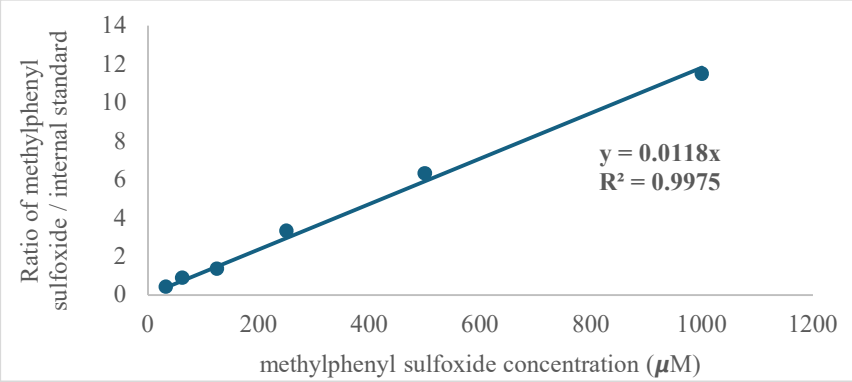



**Fig. S15** A GCMS calibration curve for the quantitation of methylphenyl sulfoxide. The curve was constructed using methylphenyl sulfoxide between 32.25-1000 µM. The calibration factor is 0.0118 $\mu M^{-1}$

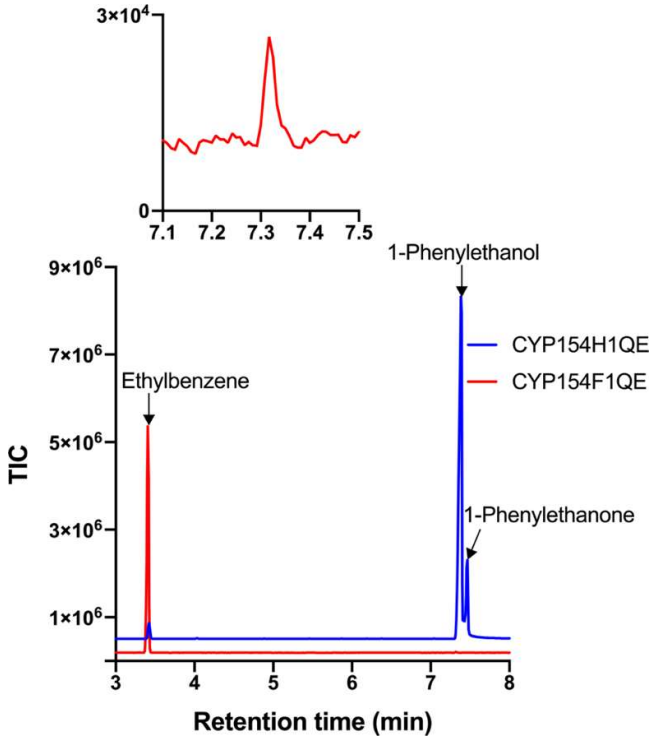
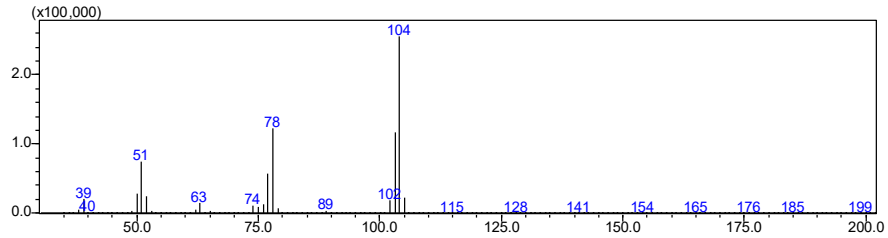


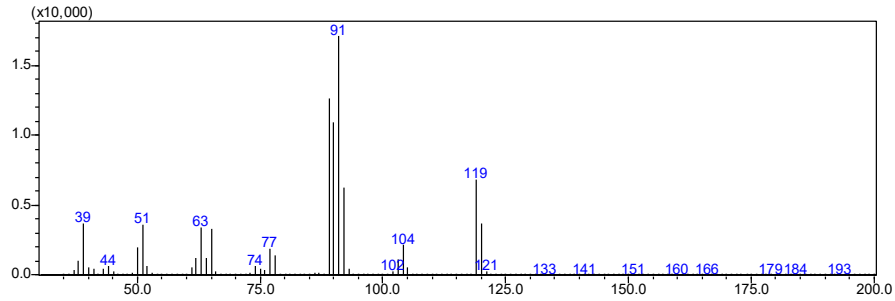

**Fig. S16** GC-MS analysis of ethylbenzene oxidation using CYP154H1QE and CYP154F1QE from *T. fusca.* The reaction contained 3 µM enzyme, 10 mM substrate and 10 mM $H_2O_2$ for 24 h. CYP154F1QE reaction (graph insert, in red) contained 3 µM enzyme, 10 mM substrate 5 mM $H_2O_2$

**Table S3.** Product distribution for the oxidation of styrene, ethylbenzene and thioanisole, catalysed by CYP154H1QE, CYP154G1QE and CYP154G1QE.

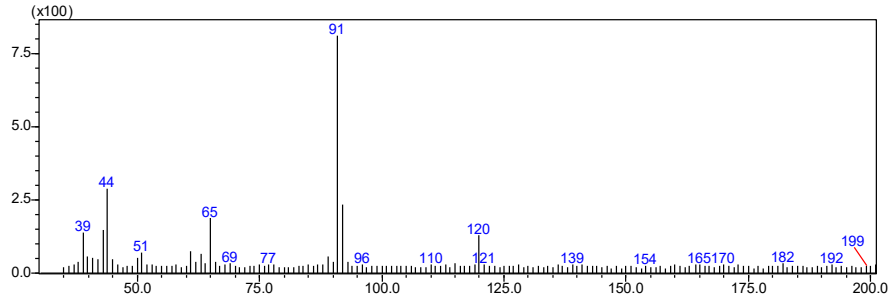
| Products | Selectivity of products generated (%) | | |
|---|---|---|---|
| | CYP154H1QE | CYP154G1QE | CYP154F1QE |
| | Styrene oxidation | | |
| Styrene oxide | 97 ± 1 | 90 ± 1 | 77 ± 2 |
| Benzaldehyde | 0.4 ± 0.001 | 4 ± 2 | 15 ± 2 |
| Phenylacetaldehyde | 2.6 ± 0.05 | 6 ± 0.3 | 8 ± 0.5 |
| | Ethylbenzene oxidation | | |
| 1-phenylethanol | 85 ± 3 | - | 100 |
| 1-phenylethanone | 15 ± 3 | - | - |
| | Thioanisole oxidation | | |
| Phenyl methyl sulfoxide | 99 ± 0.4 | 1 ± 0.4 | - |
| Phenyl methyl sulfone | 99 ± 3 | 1 ± 0.4 | - |



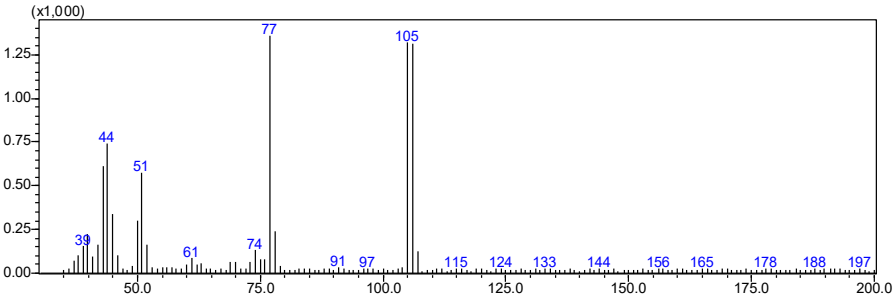

styrene RT 4.06 min




styrene oxide (phenyl oxirane) RT 7.40 min [2, 3].




phenylacetaldehyde RT 7.05 min [2, 3].




benzaldehyde RT 5.46 min [4].

**Fig. S17** The mass spectra of generated products from styrene oxidation by CYP154 enzymes

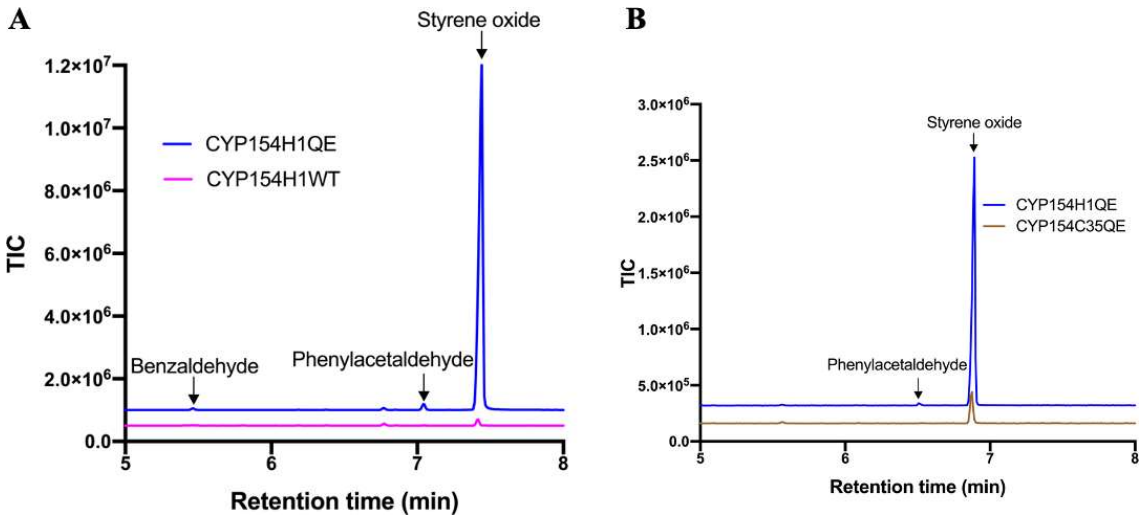
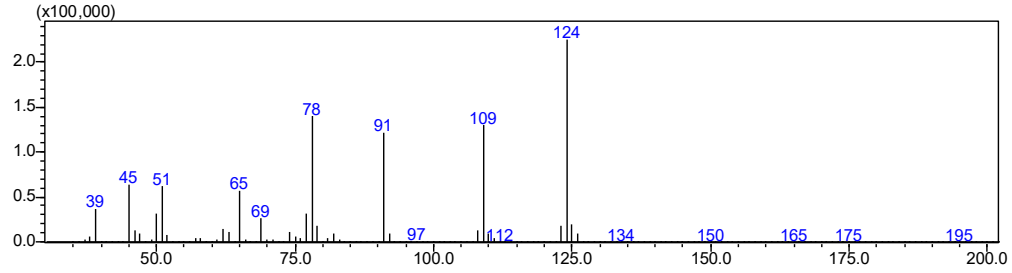
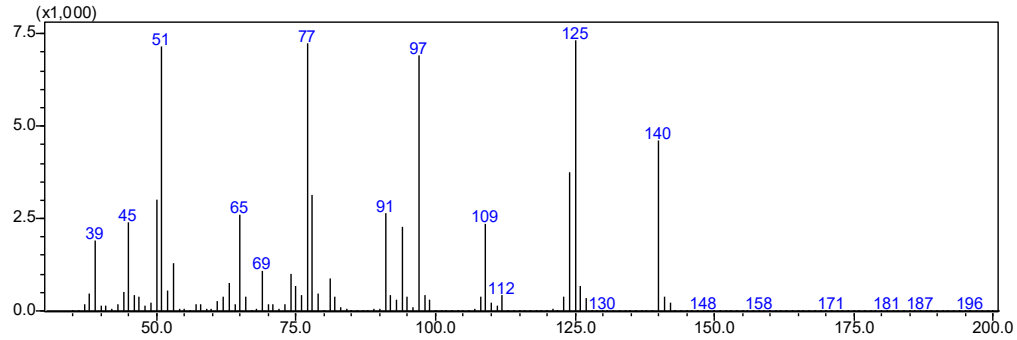


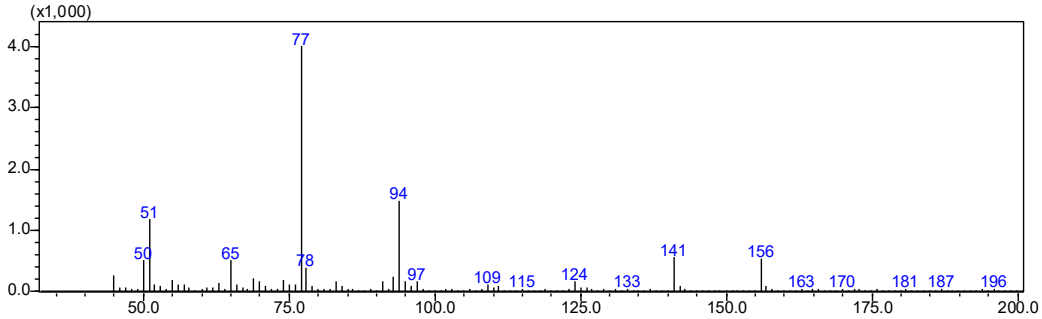

**Fig. S18** Investigation of styrene oxidation by CYP154s. The reaction mixture contained 3 µM of the respective enzymes in Tris-HCl buffer pH 7.4, 10 mM substrate and 10 mM $H_2O_2$ for 24 h




Thioanisole RT 7.84 min




methyl phenyl sulfoxide RT 11.64 min [2, 3].




methyl phenyl sulfone RT 12.77 min[2, 3].

**Fig. S19** The mass spectra of generated products from thioanisole oxidation by CYP154 enzymes

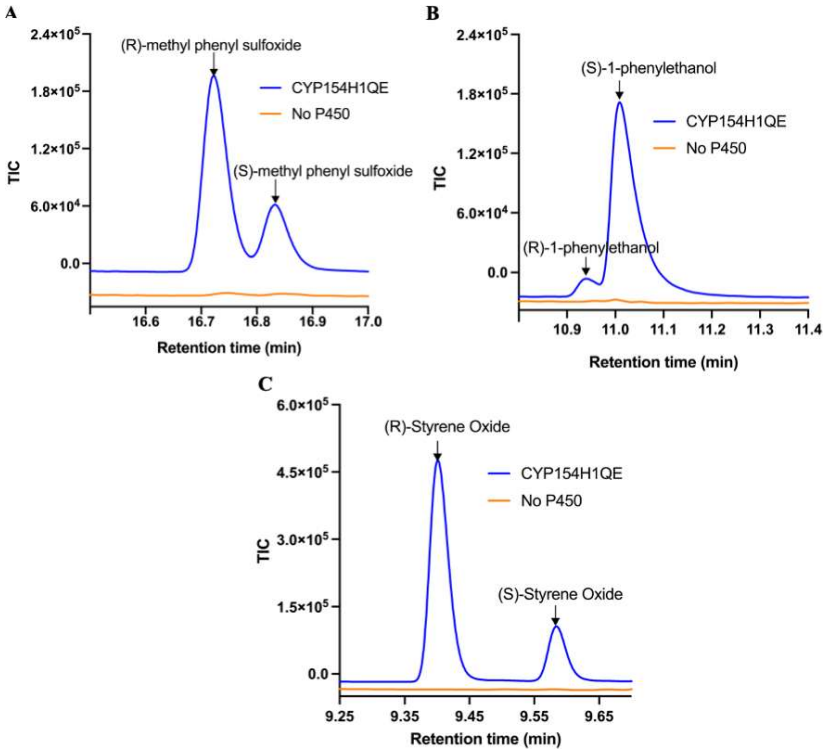



**Fig. S20** Enantioselective GC analysis of the oxidation products generated from CYP154H1QE catalysed oxidation. Oxidation of (**A**) thioanisole, (**B**) ethylbenzene and (**C**) styrene. Chiral products were identified from elution of authentic enantiopure standards under similar conditions

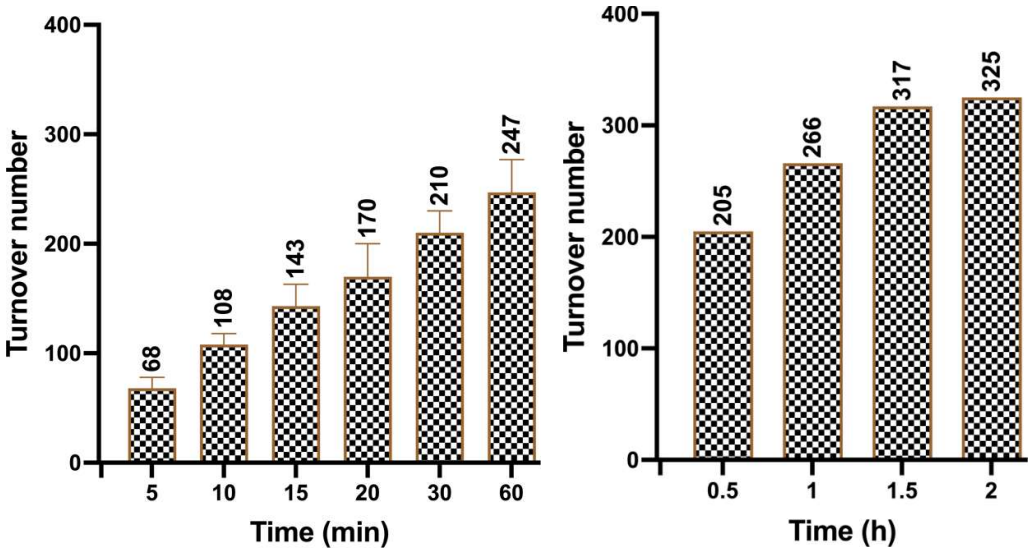



**Fig. S21** Time-course experiments of ethylbenzene oxidation by CYP154H1QE over 1 h and 2 h, respectively. The reaction mixture contained 2 μM enzyme, 10 mM ethylbenzene and 2 mM $H_2O_2$. TON is defined as the number of substrate oxidations per μM of CYP, calculated as the sum of generated 1-phenylethanol plus two equivalents of acetophenone. The amount contributed by acetophenone at increased from 0-5%, during these reactions

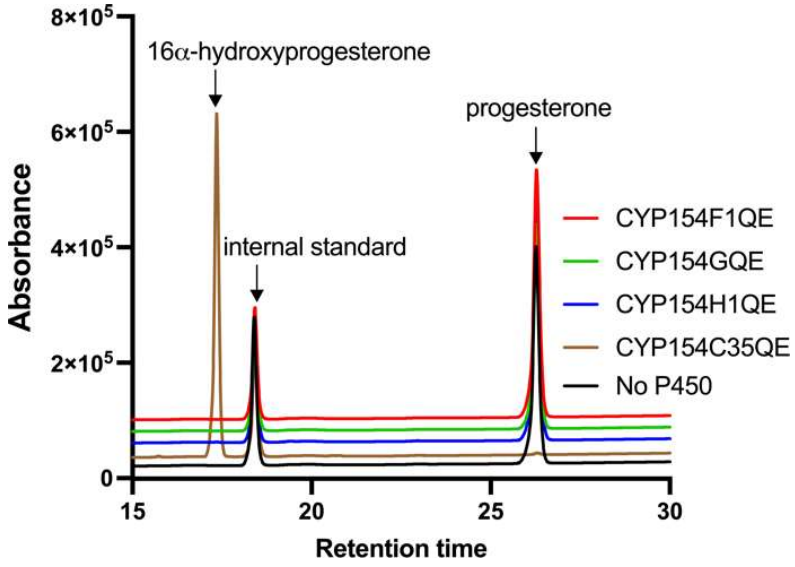
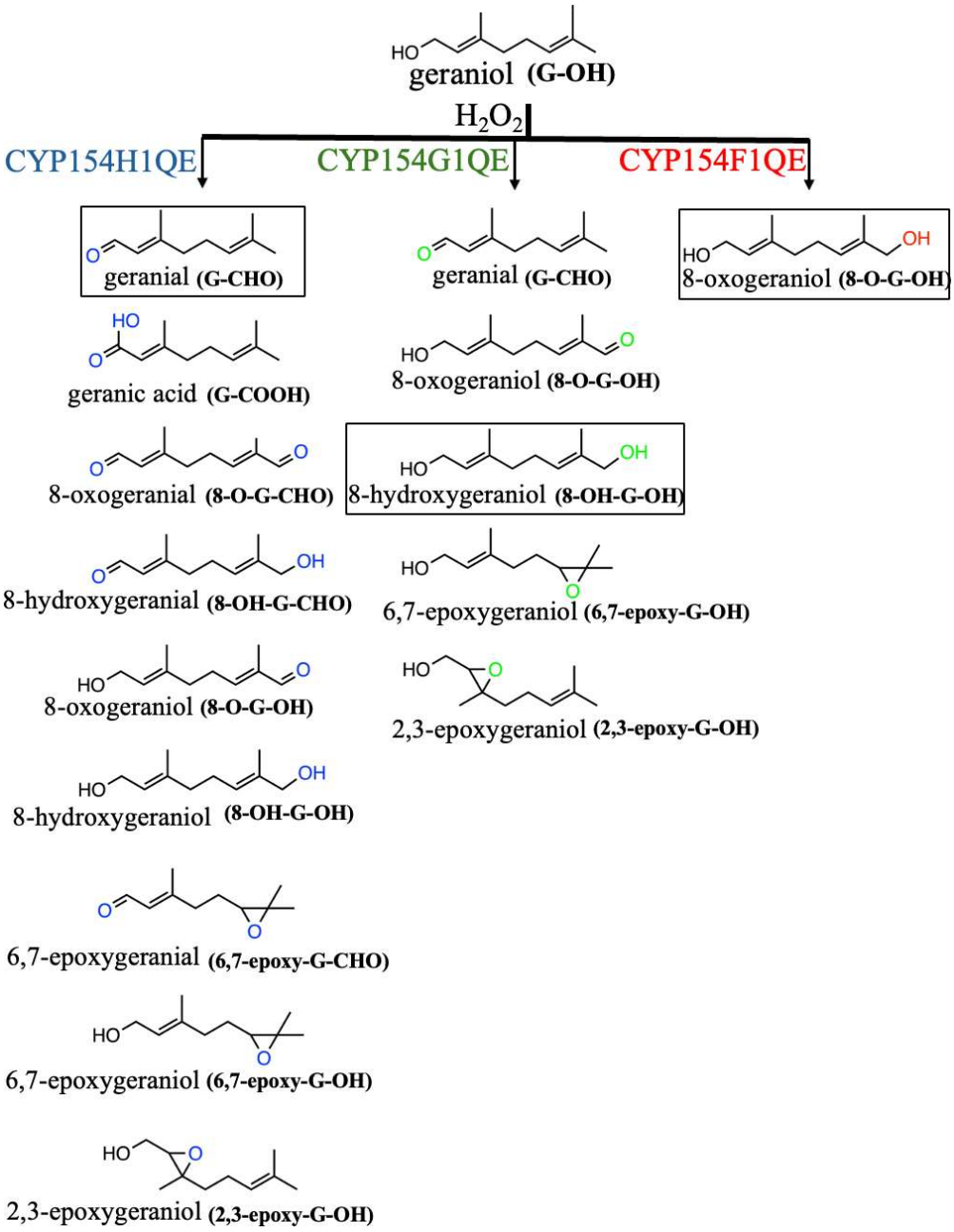
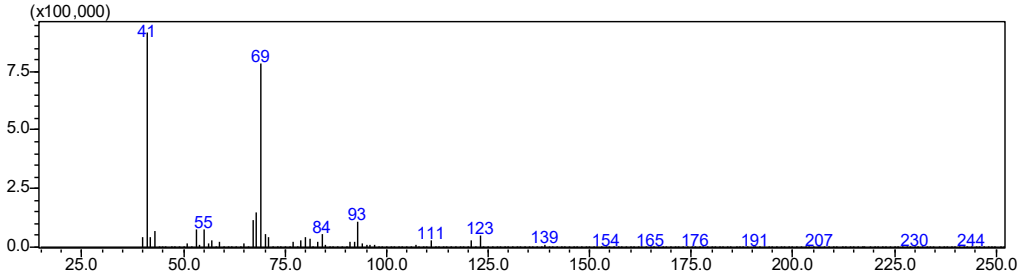


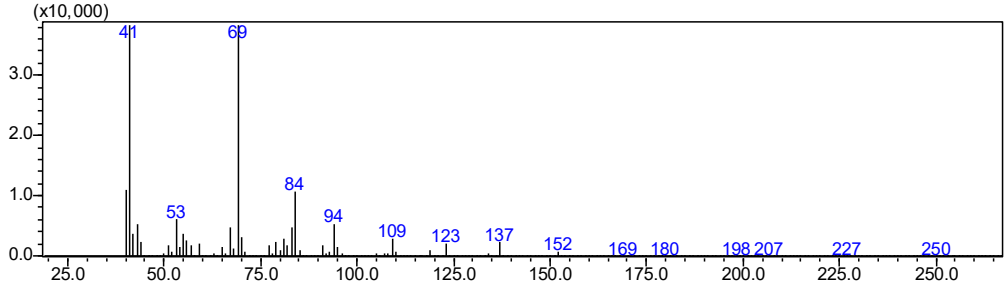

**Fig. S22** Investigation of progesterone oxidation by mutant CYP154s. The reaction mixture contained 1 μM of the respective enzymes in Tris-HCl buffer pH 7.4, 500 μM progesterone and 10 mM $H_2O_2$



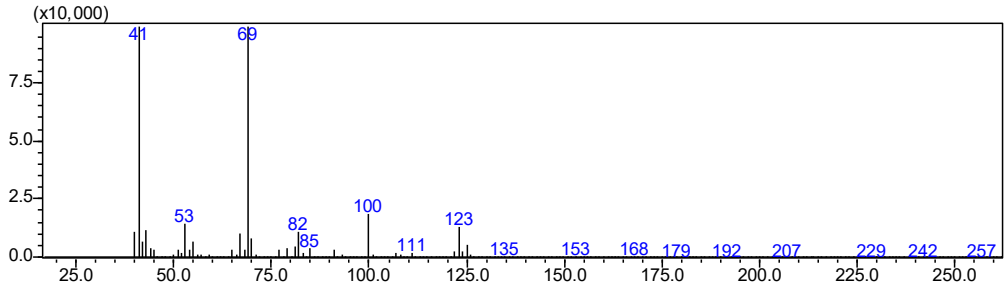

**Scheme S1.** Products generated form geraniol oxidation by CYP154H1QE, CYP154G1QE and CYP154F1QE (major products are boxed). Products were identified by matching with NIST library and comparison with published mass spectra data, see Figures S20-S22 [5-7]




geraniol RT 3.77 min

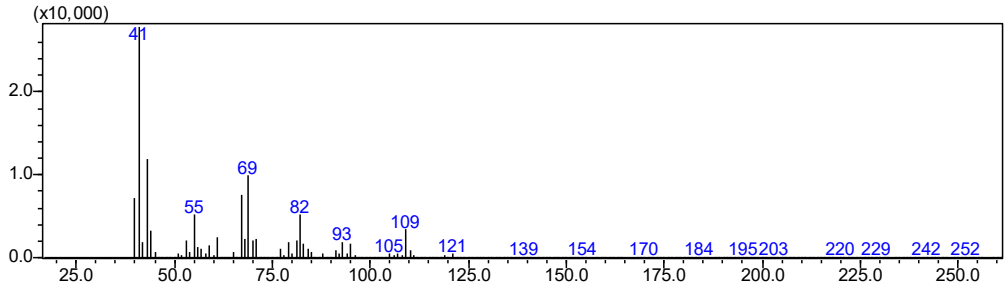



geranial RT 4.15 min

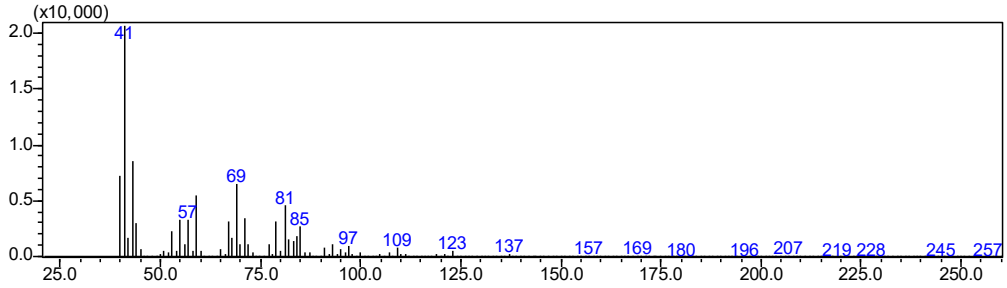



geranic acid RT 5.30 min

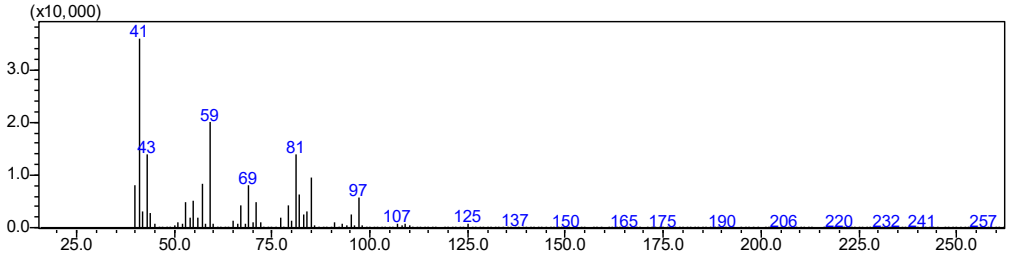
**Fig. S23** The mass spectra of generated geranial and geranic acid from geraniol oxidation by CYP154 enzymes




2,3-epoxygeraniol RT 5.12 min [5]

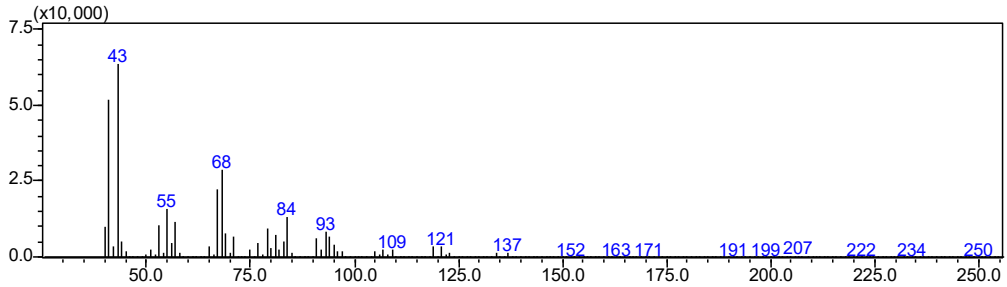



6,7-epoxygeraniol RT 5.52 min [5]

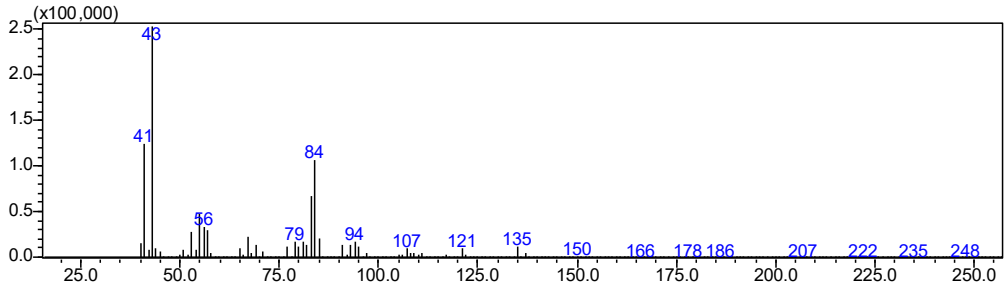



6,7-epoxygeranial RT 5.73 min

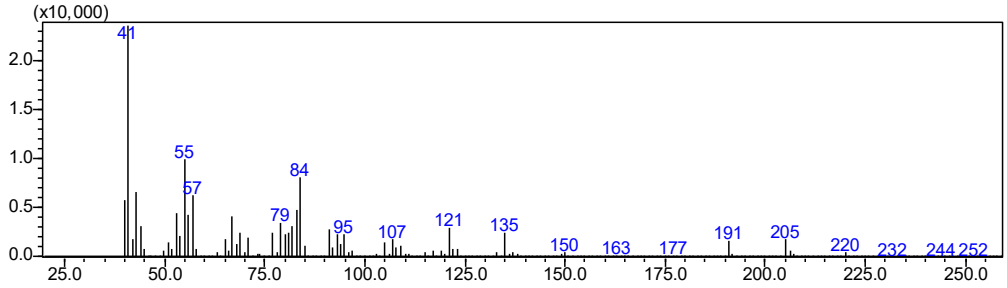
**Fig. S24** The mass spectra of generated epoxides from geraniol oxidation by CYP154 enzymes



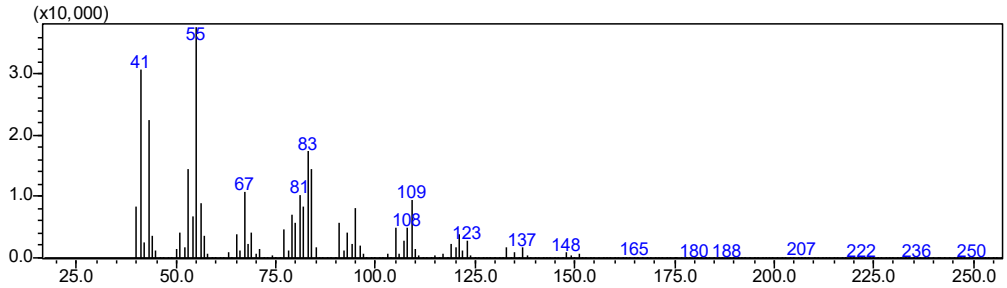

8-hydroxygeraniol RT 7.99 min [6, 7]




8-hydroxygeranial RT 8.47 min [6]




8-oxogeraniol RT 7.88 min [6].




8-oxogeranial RT 8.19 min [6].

**Fig. S25** The mass spectra of the 8-oxo and 8-hydroxy metabolites from geraniol oxidation by CYP154 enzymes

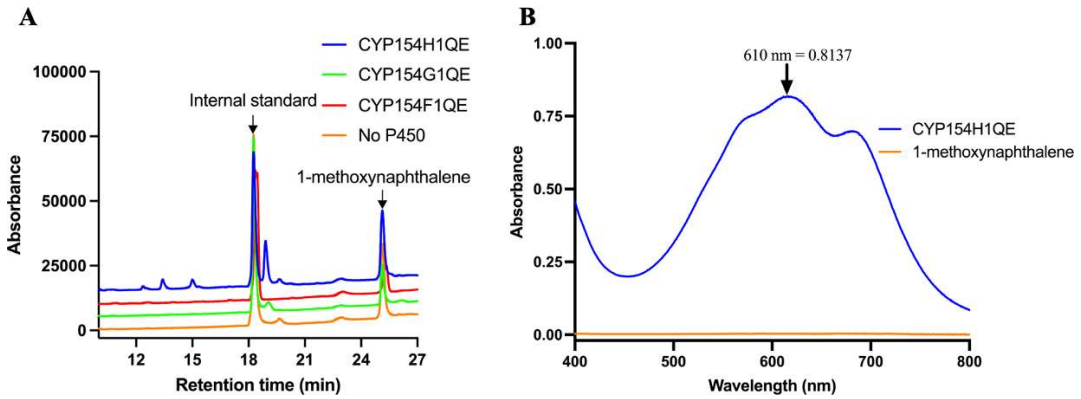
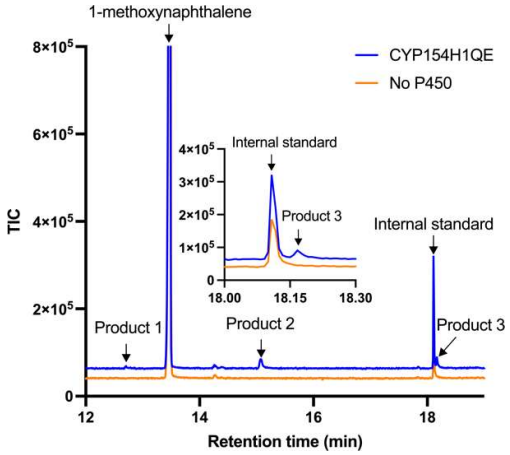


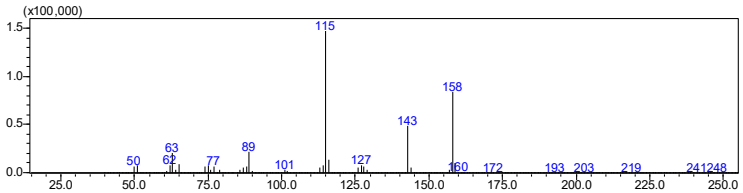

**Fig. S26** Analysis of the oxidation reactions of 1-methoxynaphthalene. (**A**) HPLC analysis of reactions with CYP154H1QE (blue), CYP154G1QE (green) and CYP154F1QE (red). (**B**) UV-Vis spectrum of CYP154H1QE catalysed oxidation of 1-methoxynaphthalene. The amount of Russig's blue generated was calculated using an extinction coefficient of 1.45 x $10^4$ $M^{-1}$ $cm^{-1}$ at 610 nm in aqueous solution [8-10]



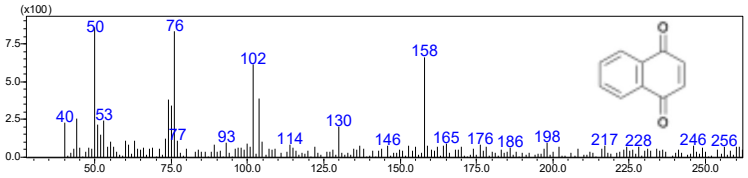

**Fig. S27** The coloured metabolite generated by CYP154H1QE reaction with indole and 1-methoxynaohthalene



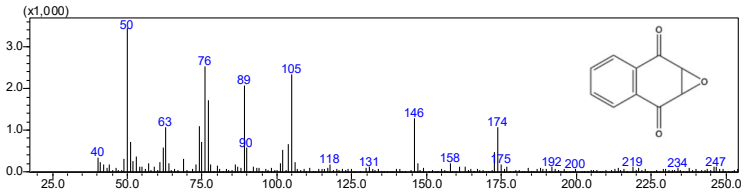

GCMS analysis of 1-methoxynaphthalene oxidation by CYP154H1QE. The reaction mixture contaned 1 mM 1-methoxynaphthalene, 1 µM CYP154H1QE and 10 mM $H_2O_2$ for 24 h



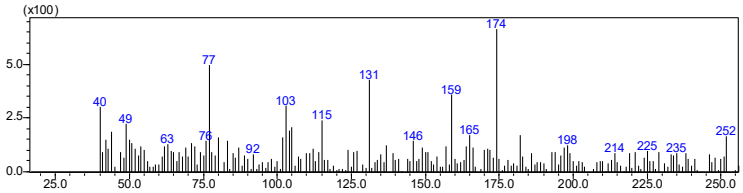
1-methoxynaphthalene (158 g/mol)



Peak 1 (RT. 12.7 min). Demethylated and further oxidised metabolite (1,4-naphthalenedione)

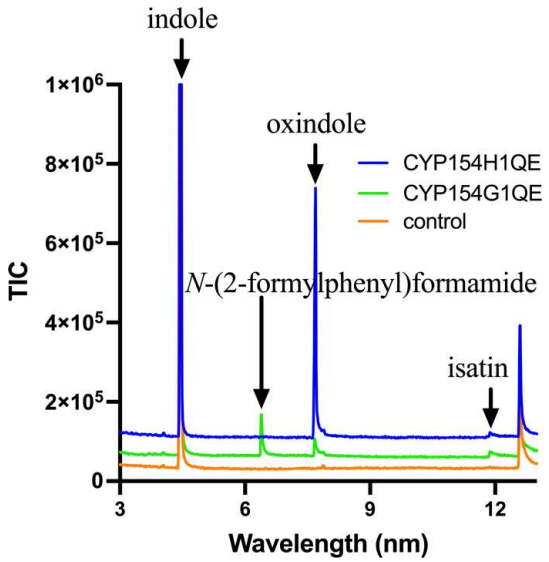


Peak 1 (RT. 15.06 min). Consistent with an oxidised metabolite of 1-methoxynaphthalene, similar to the mass spectrum of naphtho[2,3-b]oxirene-2,7-dione (NIST)

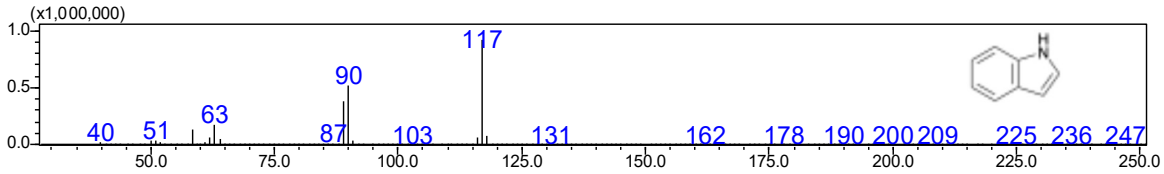


Peak 2 (RT.18.17 min) Hydroxylated derivative of 1-methoxynaphthalene

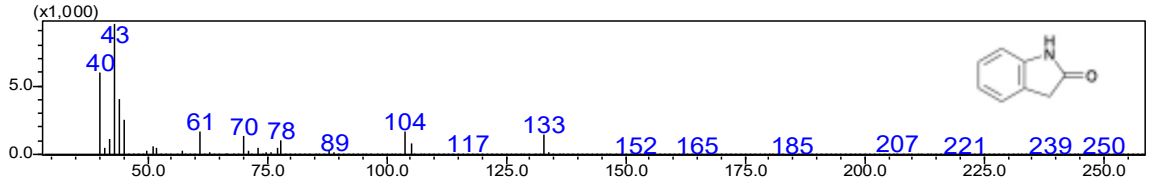
**Fig. S28** The GCMS chromatogram and mass spectra of generated metabolites from 1-methoxynaphthalene oxidation by CYP154 enzymes



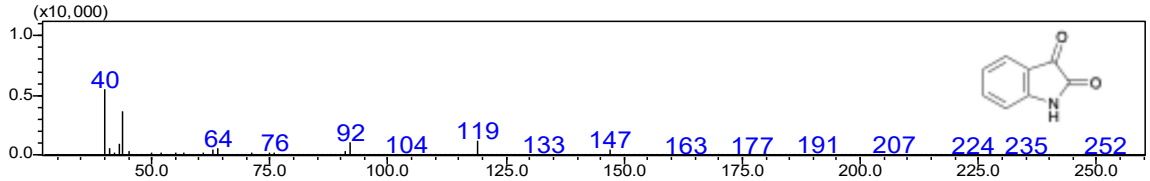

GCMS analysis of indole oxidation by CYP154 enxymes. The reaction mixture contaned 1 mM substrate, 1 μM CYP154H1QE or 3 μM CYP154G1QE and 10 mM $H_2O_2$ for 24 h.



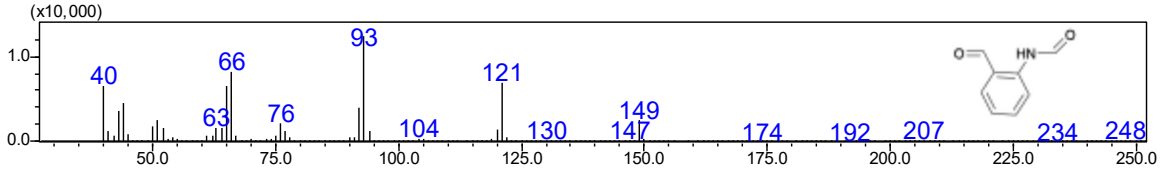

indole




oxindole RT 7.7 min [11]




isatin RT 11.9 min




*N*-(2-formylphenyl)formamide RT 6.4 min. The spectrum matched that on the Wiley and Sons Database as recorded on CAS library (CAS 25559-38-0).

**Fig. S29** The GCMS chromatogram and mass spectra of generated metabolites from indole oxidation by CYP154 enzymes

**Table S4.** Major product distribution for the oxidation of oxindole catalysed by CYP154H1QE, CYP154G1QE and CYP154G1QE. Products amounts are in µM per µM of enzyme.

| Enzyme | Oxindole | Isatin | % oxindole: isatin |
|---|---|---|---|
| CYP154H1QE | 381 ± 90 | 121 ± 10 | 76%: 24% |
| CYP154G1QE | 16 ± 6 | 24 ± 7 | 39%: 61% |
| CYP154F1QE | 17 ± 3 | 25 ± 5 | 40%: 60% |

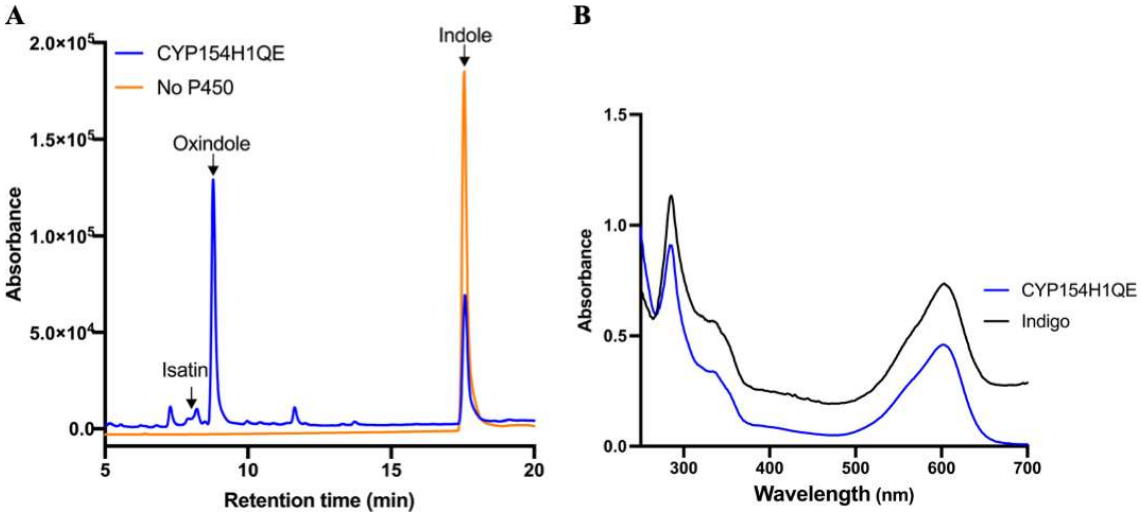



**Fig. S30** HPLC chromatogram and UV analysis of CYP154H1QE indole oxidation reaction. (**A**). Reaction contained 0.5 µM enzyme, 1 mM substrate and 10 mM $H_2O_2$. The control reaction contained a similar mixture without the enzyme (**B**). UV-Vis spectrum of indigo precipitate of CYP154H1QE reaction with spectrum of authentic indigo. The reaction contained 1 µM enzyme, 1 mM substrate and 10 mM $H_2O_2$ for 24 h

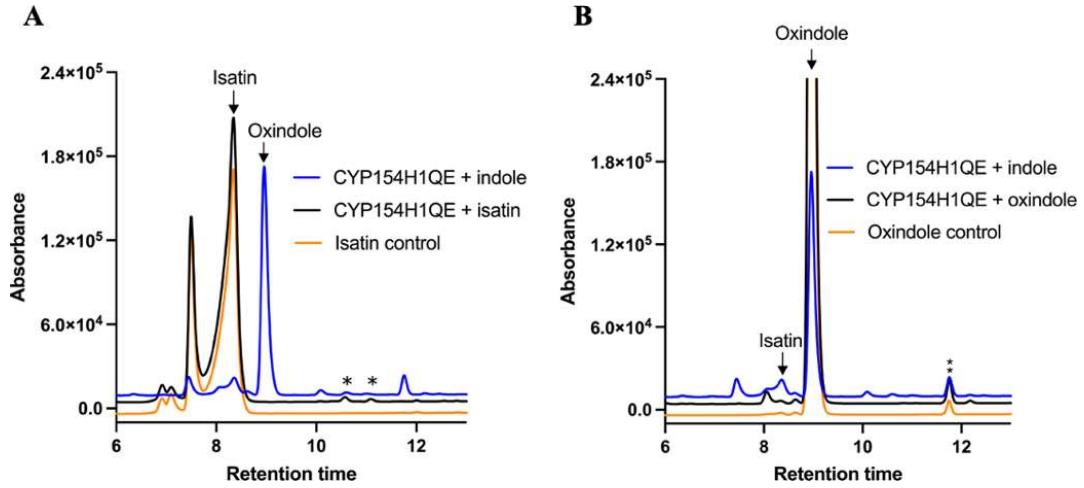



**Fig. S31** Analysis of the products of CYP154H1QE indole oxidation reaction. (**A**) CYP154H1QE indole oxidation reaction compared with CYP154H1QE (1 µM) oxidation of isatin (1 mM), driven by 10 mM $H_2O_2$. (**B**). CYP154H1QE (1 µM) oxidation of oxindole (1 mM), driven by 10 mM $H_2O_2$

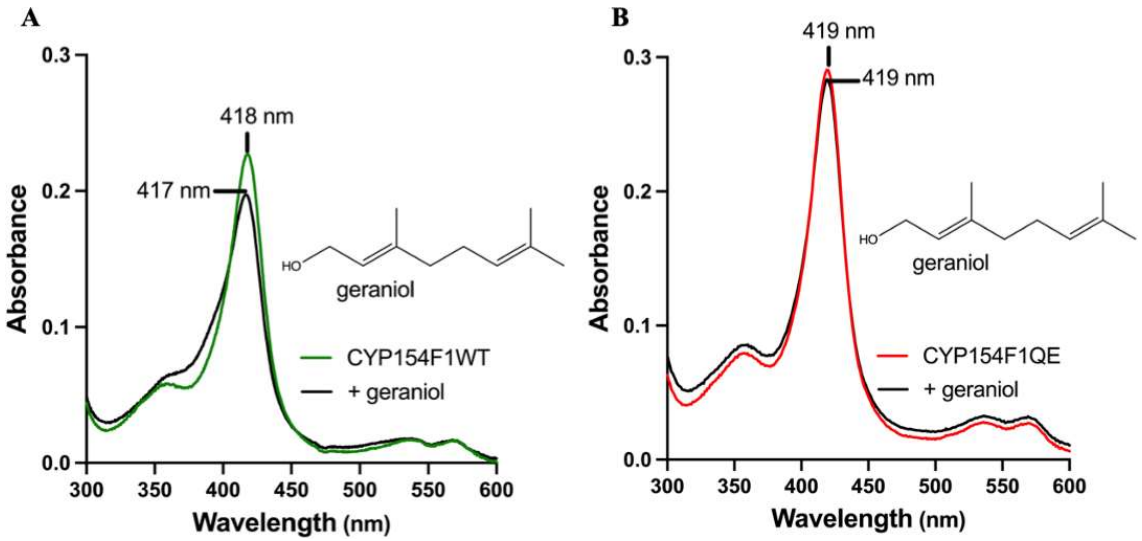



**Fig. S32** UV-Vis absorbance spectra of CYP154F in the presence or absence of geraniol. The reaction mixture contained 2 μM of **A**. CYP154F1WT (green) or **B**. CYP154F1QE (red) and 1 mM geraniol (black)

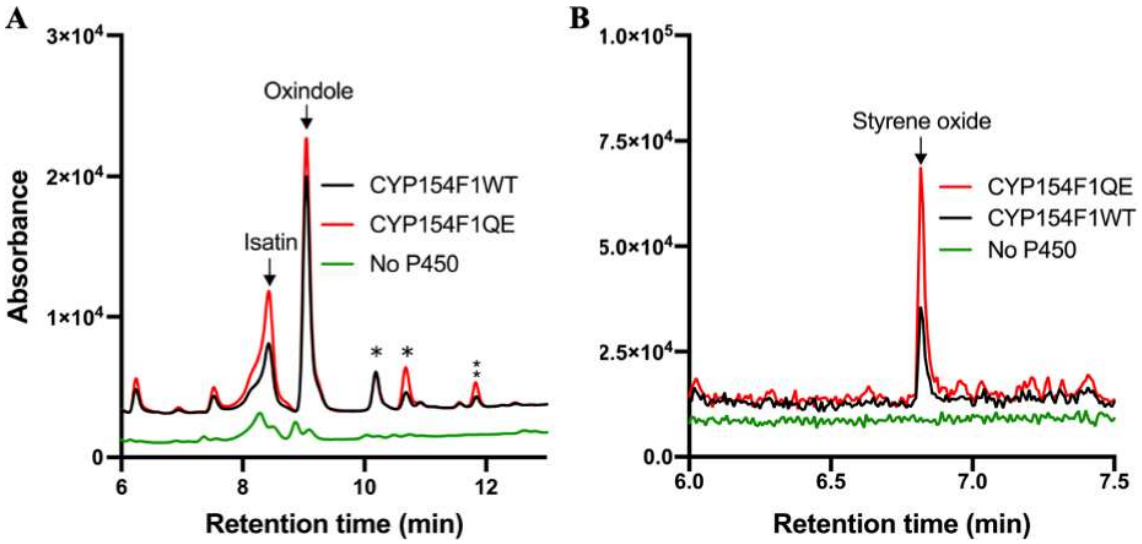
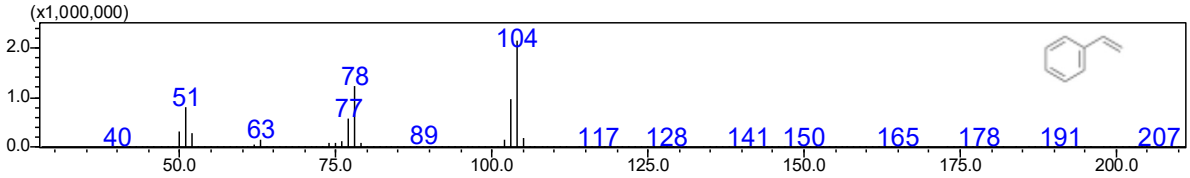
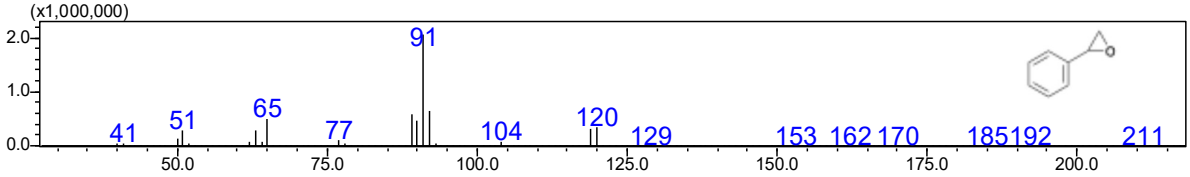


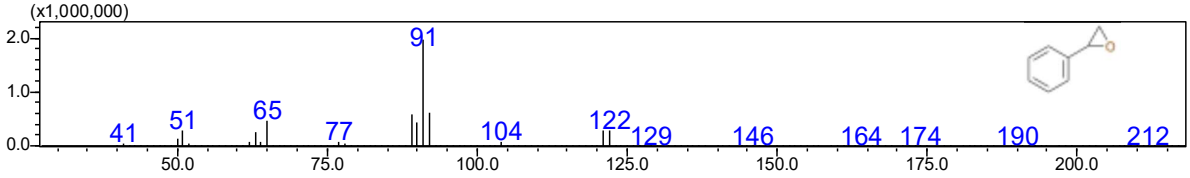

**Fig. S33** HPLC and GCMS chromatograms for the oxidation of indole and styrene by CYP154F1WT and CYP154F1QE. The reaction mixture contained 3 μM enzyme, 5 mM $H_20_2$ and either 1 mM indole or 10 mM styrene for 24 h. In styrene and indole oxidation, there was as increase of in activity of ~8% (1.1-fold) and ~226% (3.3-fold), respectively, of CYP154F1QE over WT CYP154F1. The ratio of styrene oxide versus internal standard of WT CYP154F1 was taken as 100%. The ratio amount of oxindole plus isatin generated by the WT CYP154F1 as 100%. The oxindole: isatin ratio of WT CYP154F1 was 76%: 24% (that of the QE variant was 40%: 60%, respectively)



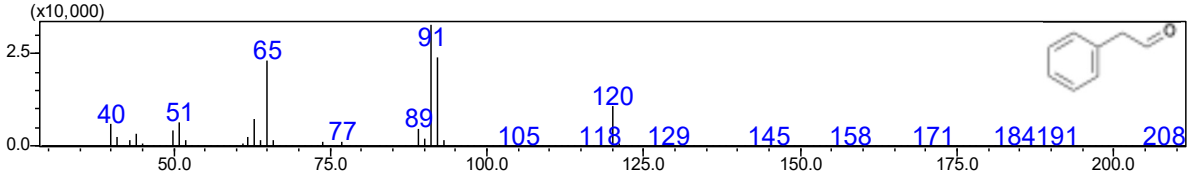

styrene



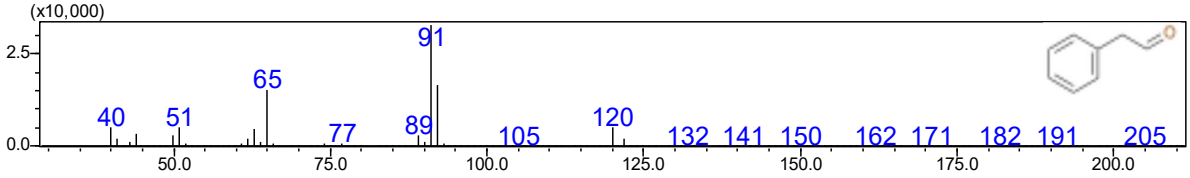

styrene oxide in control $H_2O_2$ reaction




styrene oxide with $^{18}O$ atom incorporated from $^{18}O$ labelled $H_2O_2$

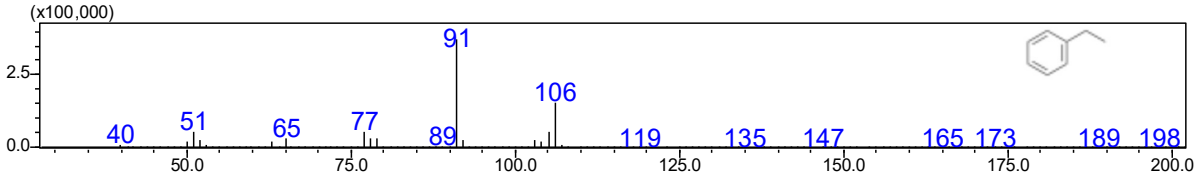



phenylacetaldehyde in control $H_2O_2$ reaction

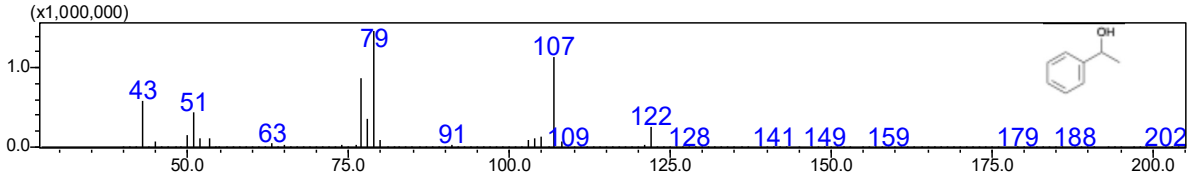



phenylacetaldehyde with $^{18}O$ atom incorporated from $^{18}O$ labelled $H_2O_2$

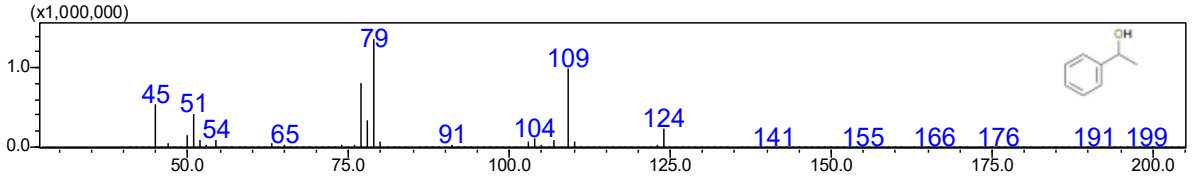
**Fig. S34** GC-MS analysis of styrene oxidation by CYP154H1QE using $^{18}O$ labelled $H_2O_2$. The reaction mixture contained 10 mM substrate, 3 µM enzyme and 2 mM $^{18}O$ labelled $H_2O_2$. Control reactions were carried out in identical conditions with non-labelled $H_2O_2$. Phenylacetaldehyde as a smaller peak at mass 122 as it can form an equilibrium with a gem-diol which in water would replace $^{18}O$ with unlabelled O from water



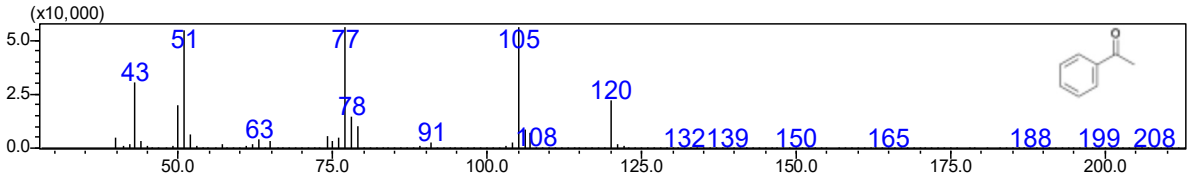

ethylbenzene



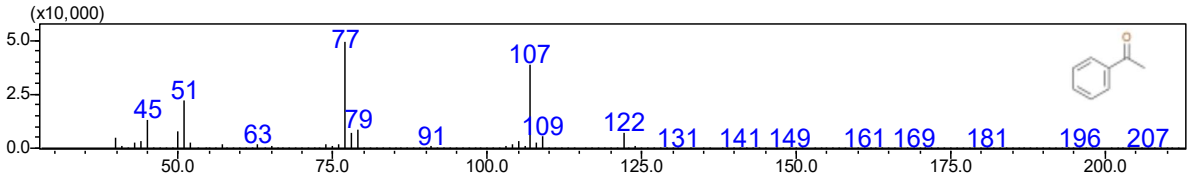

1-phenylethanol in control $H_2O_2$ reaction




1-phenylethanol with $^{18}O$ atom incorporated from $^{18}O$ labelled $H_2O_2$

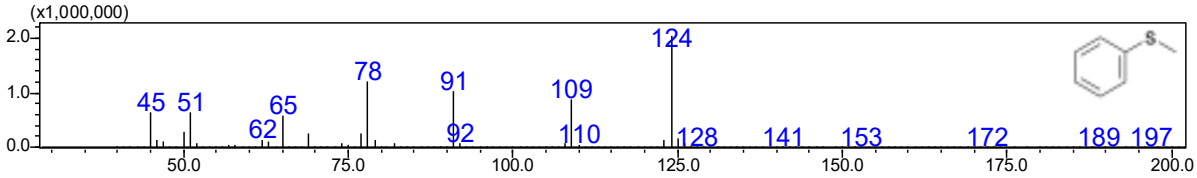



acetophenone in control $H_2O_2$ reaction

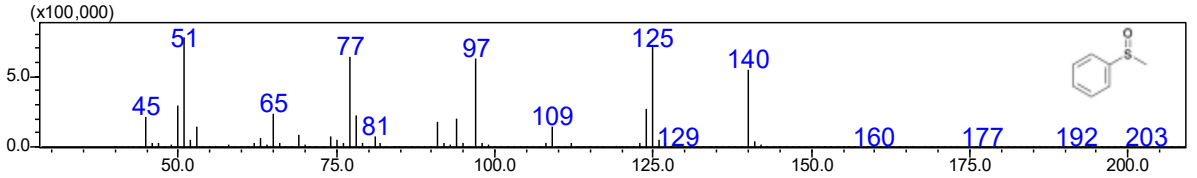



acetophenone $^{18}O$ atom incorporated from $^{18}O$ labelled $H_2O_2$.

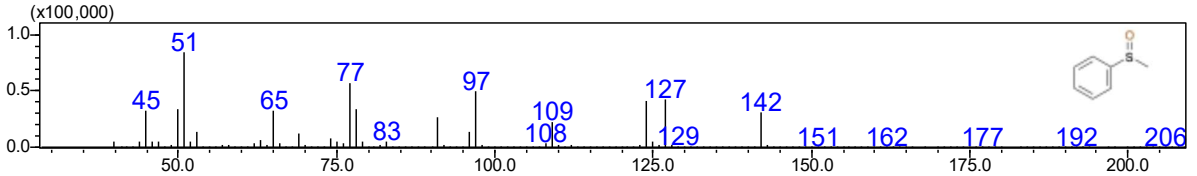
**Fig. S35** GC-MS analysis of ethylbenzene oxidation by CYP154H1QE using $^{18}O$ labelled $H_2O_2$. The reaction mixture contained 10 mM substrate, 3 μM enzyme and 2 mM $^{18}O$ labelled $H_2O_2$. Control reactions were carried out in identical conditions with non-labelled $H_2O_2$




thioanisole

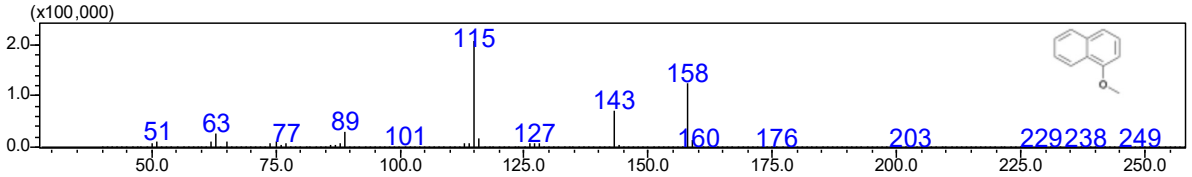



phenyl methyl sulfoxide in control $H_2O_2$ reaction

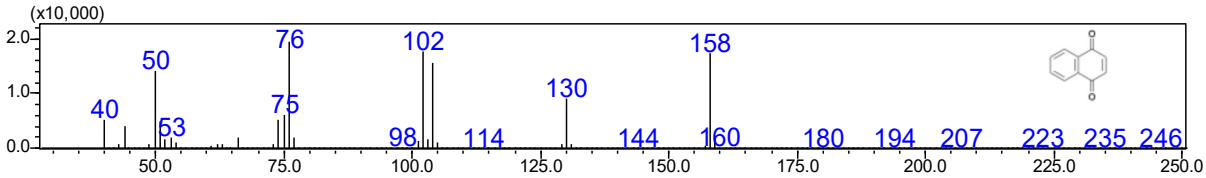



phenyl methyl sulfoxide $^{18}O$ atom incorporated from $^{18}O$ labelled $H_2O_2$.

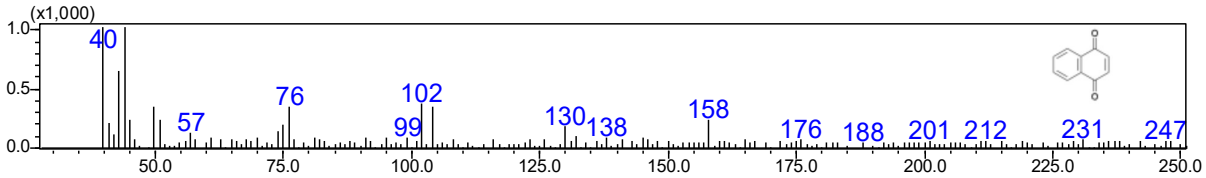
**Fig. S36** GC-MS analysis of thioanisole oxidation by CYP154H1QE using $^{18}O$ labelled $H_2O_2$. The reaction mixture contained 1 mM substrate, 3 µM enzyme and 2 mM $^{18}O$ labelled $H_2O_2$. Control reactions were carried out in identical conditions with $H_2O_2$



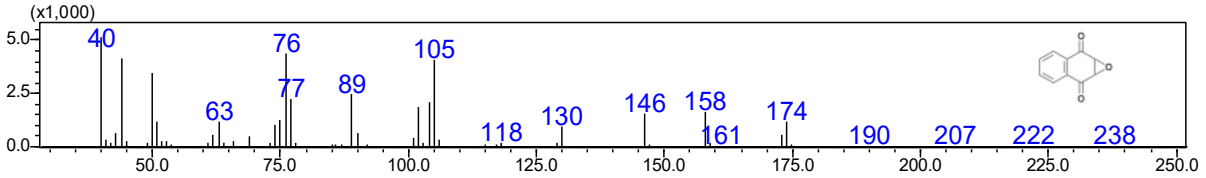

1-methoxynaphthalene



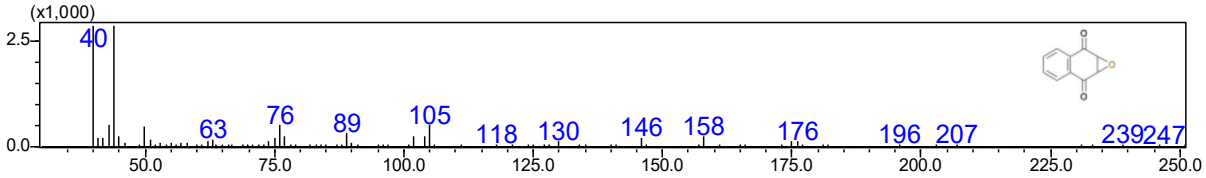

1,4-naphthalenedione in CYP154H1QE supported by control $H_2O_2$. (NIST)[11]




1,4-Naphthalenedione. Enzyme catalysed demethylation followed by metabolite autoxidation. MS same in $^{18}O$ labelled $H_2O_2$ and control $H_2O_2$ reaction.

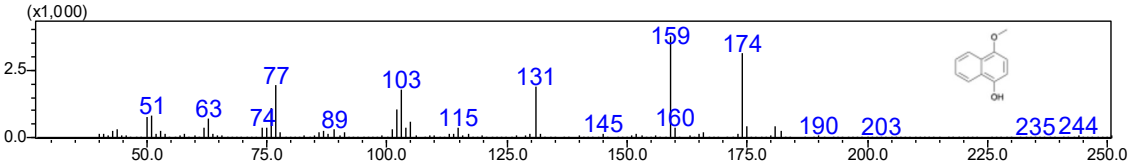



Oxidised metabolite in control $H_2O_2$ reaction

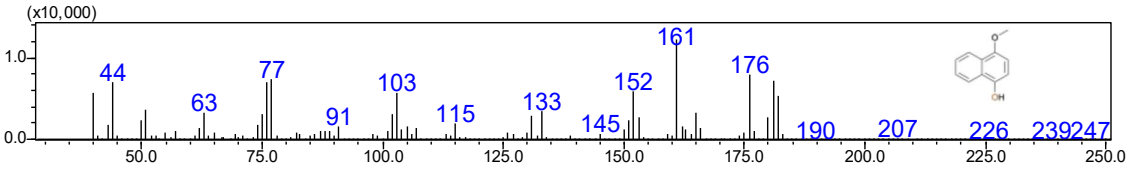



Oxidised metabolite with $^{18}O$ atom incorporated from $^{18}O$ labelled $H_2O_2$

**Fig. S37** GC-MS analysis of 1-methoxynaphthalene oxidation by CYP154H1QE using $^{18}O$ labelled $H_2O_2$. The reaction mixture contained 1 mM substrate, 2 µM enzyme and 2 mM $^{18}O$ labelled $H_2O_2$. Control reactions were carried out in identical conditions with $H_2O_2$

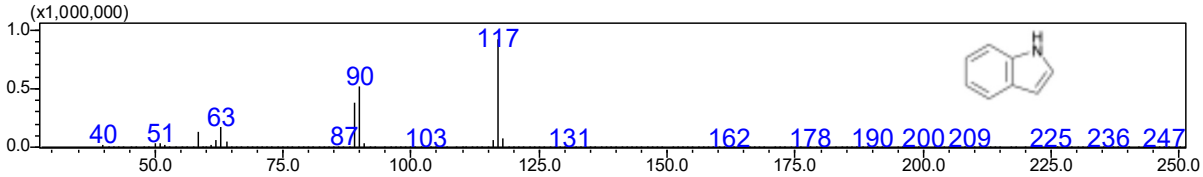



Hydroxylated metabolite (4-methoxy-1-naphthol) in control $H_2O_2$ reaction [12]

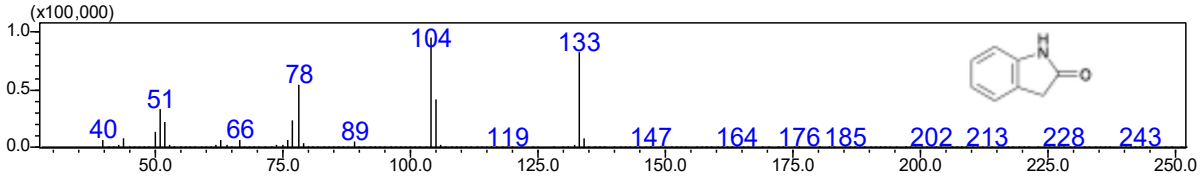



4-methoxy-1-naphthol with $^{18}O$ atom incorporated from $^{18}O$ labelled $H_2O_2$

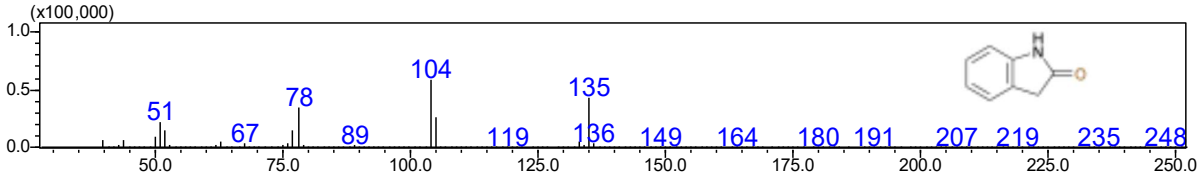
**Fig. S38** MS of hydroxylated metabolite from oxidation of 1-methoxynaphthalene by CYP154H1QE using $^{18}O$ labelled $H_2O_2$. The reaction mixture contained 1 mM substrate, 2 µM enzyme and 2 mM $^{18}O$ labelled $H_2O_2$. Control reactions were carried out in identical conditions with $H_2O_2$



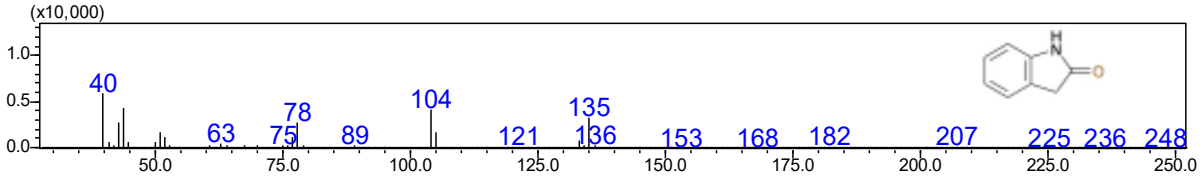

indole



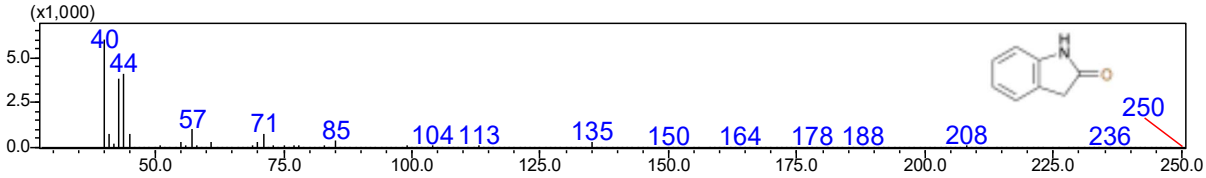

oxindole in control reaction with enzyme and non-labelled $H_2O_2$ reaction [11]




oxindole in CYP154H1QE reaction supported by $^{18}O$ labelled $H_2O_2$.$^{18}O$ atom incorporated

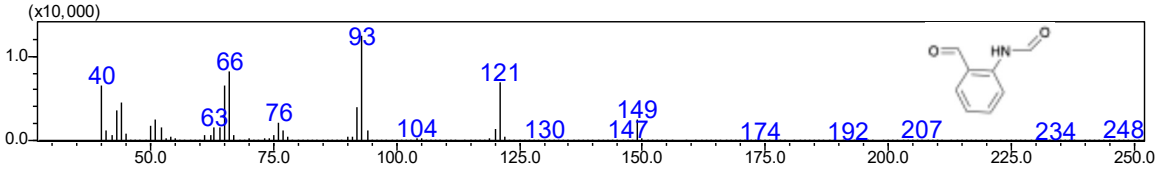



oxindole in CYP154G1QE reaction supported by $^{18}O$ labelled $H_2O_2$.$^{18}O$ atom incorporated

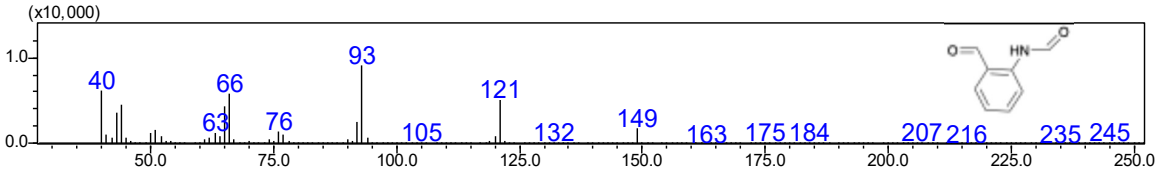



oxindole in CYP154F1QE reaction supported by $^{18}O$ labelled $H_2O_2$.$^{18}O$ atom incorporated

**Fig. S39** GC-MS analysis of indole oxidation by CYP154H1QE, CYP15G1QE and CYP154F1QE using $^{18}O$ labelled $H_2O_2$. The reaction mixture contained 1 mM indole, 3 µM enzyme and 2 mM $^{18}O$ labelled $H_2O_2$. Control reactions were carried out in identical conditions with $H_2O_2$. Reactions with CYP154H1QE contained 1 µM enzyme




*N*-(2-Formylphenyl)formamide in CYP154G1QE reaction with control $H_2O_2$




*N*-(2-Formylphenyl)formamide in CYP154G1QE reaction with $^{18}O$ labelled $H_2O_2$

**Fig. S40** GC-MS analysis of indole oxidation by CYP15G1QE at 3 μM concentration. RT 6.4 min, oxindole eluted at 7.2 min

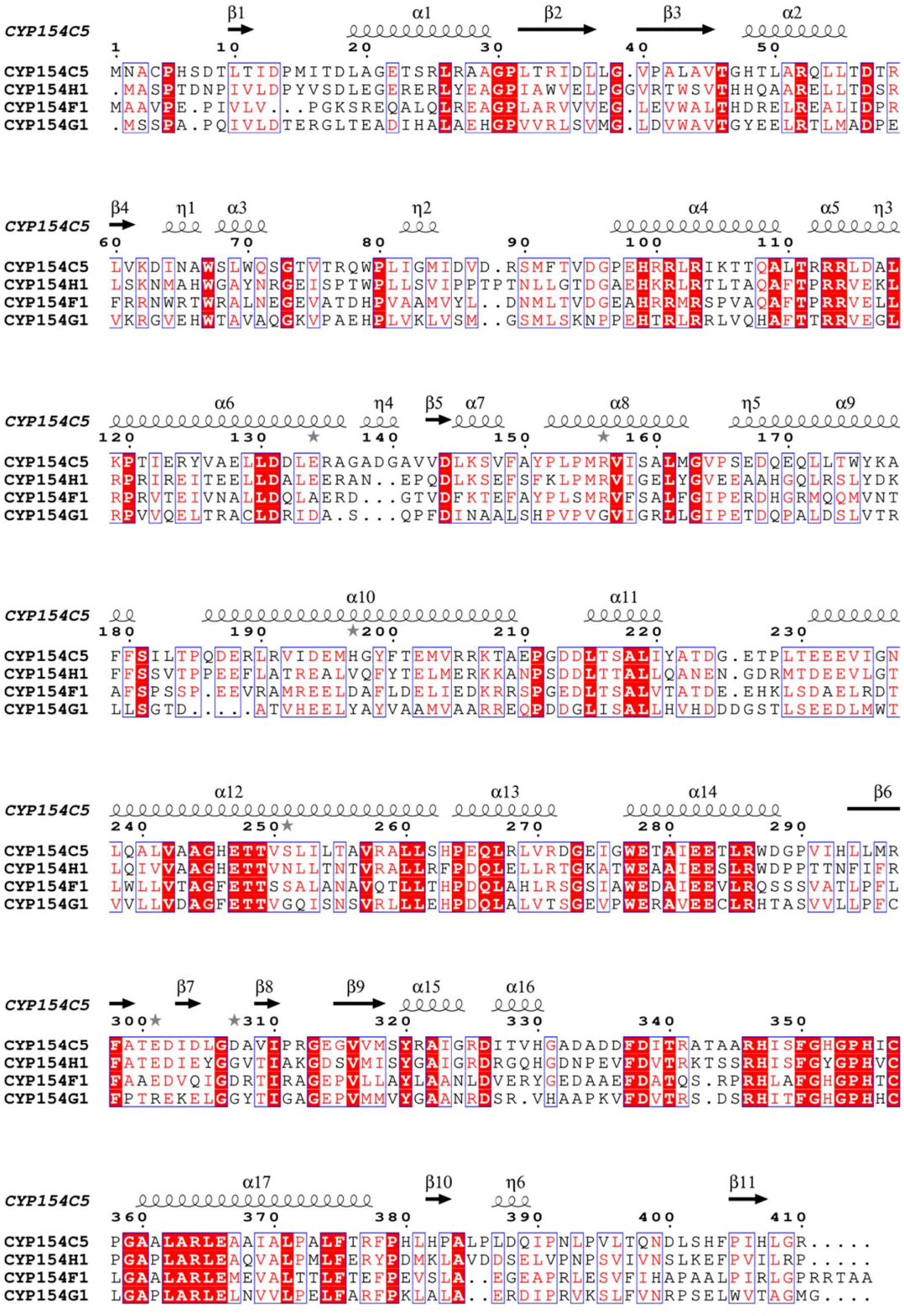



**Fig. S41** Protein sequence alignment of CYP154H1, CYP154F1 and CYP154G1 from *T. fusca* with CYP154C5 (PDB entry 4J6C)

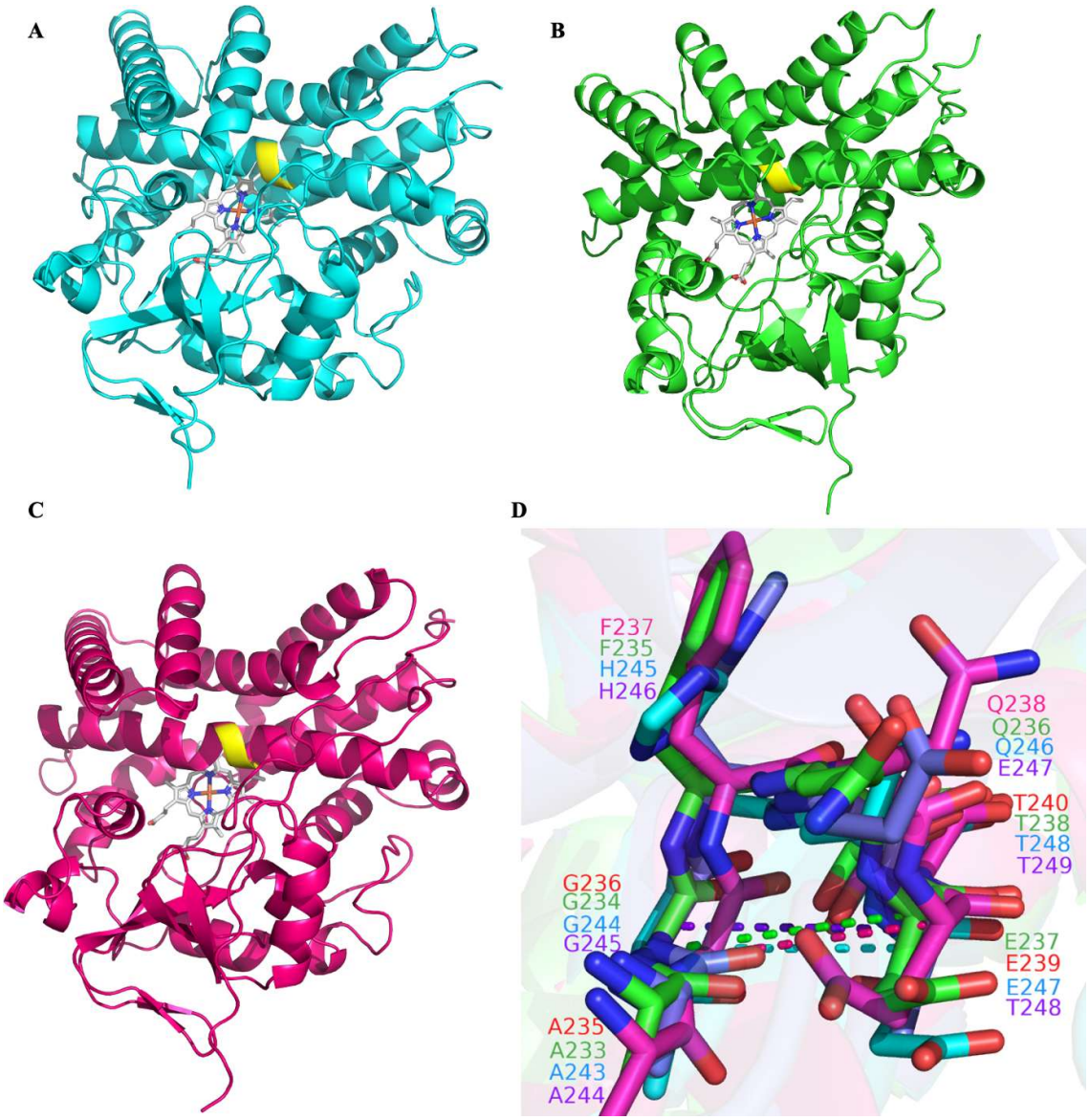



**Fig. S42** AlphaFold models of CYP154H1QE, CYP154G1QE and CYP154F1QE from *T. fusca*. (**A**) CYP154H1QE (cyan (**B**) CYP154G1QE (green) and (**C**) CYP154F1QE (Pink), QE mutations are highlighted in yellow. (**D**) Stick model of the dioxygen binding ($O_2$-binding) groove of CYP154H1QE, CYP154G1QE, CYP154F1QE, and the X-ray structure of WT CYP154C5 (PDB entry 4J6C) (purple). The $O_2$-binding groove of CYP154C5, CYP154H1QE, CYP154G1QE and CYP154F1QE

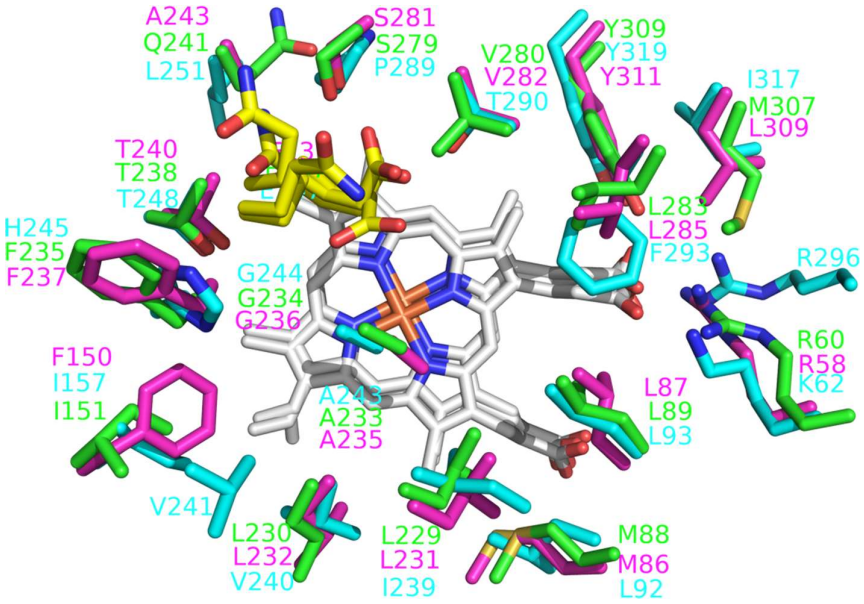



**Fig. S43** The overlay of the active site residues of CYP154H1QE, CYP154G1QE and CYP154F1QE derived from Alphafold models. CYP154H1QE (cyan), CYP154G1QE (green) and CYP154F1QE (pink)

**Table S6.** Residues above the heme and within 5 Å in CYP154C5 (PDP entry 4J6C) and the enzymes, CYP54H1, CYP154F1 and CYP154G1 from *T. fusca*. Residues which are conserved with those in CYP154C5 are in bold while the most common residue at each position in CYP154H1, CYP154G1 and CYP154F1 are underlined. * Residues may sterically clash with progesterone if the binding is in a similar position as in CYP154C5.

| CYP154C5 | CYP154H1 | CYP154G1 | CYP154F1 |
|---|---|---|---|
| **K62** | **K62** | R60 | R58 |
| **G83** | S83 | K81 | A79 |
| **M91** | L92 | **M88** | **M86** |
| **F92** | L93 | L89 | L87 |
| **I158** | **I157** | **I151** | F150 |
| **F179** | **F178*** | L172 | A171 |
| **Q239** | **Q238** | V228 | W230* |
| **A240** | I239 | L229* | L231* |
| **L241** | V240 | **L230** | **L232** |
| **A243** | **A242** | D232* | T234 |
| **A244** | **A243** | **A233** | **A235** |
| **G245** | **G244** | **G234** | **G236** |
| **H246** | **H245** | F235 | F236 |
| **E247** | **E247*** | **E236** | **E238** |
| **T248** | **T248** | **T237** | **T239** |
| **T249** | **T248** | **T238** | **T240** |
| **L252** | **L251** | Q241 | A243 |
| **P290** | **P289** | S297 | S281 |
| **V291** | T290 | **V280** | **V282** |
| **L294** | F293 | **L283** | **L285** |
| **R297** | **R296** | C289 | L291 |
| **M318** | I317 | **M307** | L309 |
| **Y320** | **Y319** | **Y309** | **Y311** |
| **Q398** | V397 | V383 | I386 |

These residues in CYP154C5 are conserved in the CYP154C35 except for I158 which is V155, in CYP154C35. This agrees with the similar substrate range of the CYP154C subfamily enzymes.

**Table S7.** Percent sequence identity matrix of CYP154 enzymes from *Thermobifida fusca* and *Nocardia otitidiscaviarum* in comparison to CYP154C5 form *Nocardia farcinica* (pdb_00004j6c) and CYP154C8 from *Streptomyces* sp.

| | **H1** | **C8** | **C5** | **C35** | **F1** | **G1** |
|---|---|---|---|---|---|---|
| **CYP154H1** | **100.00** | 50.12 | 46.81 | 49.75 | 41.21 | 37.82 |
| **CYP154C8** | 50.12 | **100.00** | 67.48 | 72.10 | 39.55 | 35.79 |
| **CYP154C5** | 46.81 | 67.48 | **100.00** | 73.65 | 40.45 | 35.79 |
| **CYP154C35** | 49.75 | 72.10 | 73.65 | **100.00** | 39.85 | 34.27 |
| **CYP154F1** | 41.21 | 39.55 | 40.45 | 39.85 | **100.00** | 40.56 |
| **CYP154G1** | 37.82 | 35.79 | 35.79 | 34.27 | 40.56 | **100.00** |

## References


1. Osiebe O, Hayball EF, Yevstigneyev N, Abbott AM, Bell SG (2026) Scalable and stereoselective C–H bond hydroxylation of steroids using a designer heme-thiolate peroxygenase biocatalyst. The Journal of Organic Chemistry 91:1165-76. https://doi.org/10.1021/acs.joc.5c02818

2. Munday SD, Dezvarei S, Bell SG (2016) Increasing the activity and efficiency of stereoselective oxidations by using decoy molecules in combination with rate-enhancing variants of P450Bm3. ChemCatChem 8:2789-96. https://doi.org/https://doi.org/10.1002/cctc.201600551

3. Dezvarei S, Shoji O, Watanabe Y, Bell SG (2019) The effect of decoy molecules on the activity of the P450Bm3 holoenzyme and a heme domain peroxygenase variant. Catalysis Communications 124:97-102. https://doi.org/https://doi.org/10.1016/j.catcom.2019.03.004

4. Ali AAQ, Siddiqui ZN (2023) Heteropoly ionic liquids functionalized γ-Fe2O3 NPs: synthesis, characterization, and catalytic application in selective oxidation of benzyl alcohol to benzaldehyde using $H_2O_2$ as a green oxidant. Research on Chemical Intermediates 49:1085-113. https://doi.org/10.1007/s11164-022-04945-w

5. Molińska Nee Sosińska E, Klimczak U, Komaszyło J, Derewiaka D, Obiedziński M, Kania M, Danikiewicz W, Swiezewska E (2016) Double bond stereochemistry influences the susceptibility of short-chain isoprenoids and polyprenols to decomposition by thermo-oxidation. Lipids 51:1323. https://doi.org/10.1007/s11745-015-4013-0

6. Miettinen K, Dong L, Navrot N, Schneider T, Burlat V, Pollier J, Woittiez L, van der Krol S, Lugan R, Ilc T, Verpoorte R, Oksman-Caldentey K-M, Martinoia E, Bouwmeester H, Goossens A, Memelink J, Werck-Reichhart D (2014) The seco-iridoid pathway from *Catharanthus roseus*. Nature Communications 5:3606. https://doi.org/10.1038/ncomms4606

7. Dusséaux S, Wajn WT, Liu Y, Ignea C, Kampranis SC (2020) Transforming yeast peroxisomes into microfactories for the efficient production of high-value isoprenoids. Proceedings of the National Academy of Sciences 117:31789-99. https://doi.org/doi:10.1073/pnas.2013968117

8. Erman JE, Kilheeney H, Bidwai AK, Ayala CE, Vitello LB (2013) Peroxygenase activity of cytochrome c peroxidase and three apolar distal heme pocket mutants: hydroxylation of 1-methoxynaphthalene. BMC Biochemistry 14:19. https://doi.org/10.1186/1471-2091-14-19

9. Kawana H, Miwa T, Honda Y, Furuya T (2022) Sustainable approach for peroxygenase-catalyzed oxidation reactions using hydrogen peroxide generated from spent coffee grounds and tea leaf residues. ACS Omega 7:20259-66. https://doi.org/10.1021/acsomega.2c02186

10. Podgorski MN, Lee JHZ, Scaffidi-Muta JM, Akter J, Bell SG (2025) Characterisation of a self-sufficient cytochrome P450 enzyme from the bacterium *Thermosporothrix hazakensis* and its conversion into a peroxygenase. Microbial Biotechnology 18:e70234. https://doi.org/10.1111/1751-7915.70234

11. Linstrom PJ, Mallard WG, editors. NIST Chemistry WebBook. Gaithersburg, MD, 20899: National Institute of Standards and Technology.

12. SDBS. National Institute of Advanced Industrial Science and Technology 2026 [Available from: https://sdbs.db.aist.go.jp/